Intelligent Reflecting Surface Assisted Secure Wireless Communications With Multiple-Transmit and Multiple-Receive Antennas

WEIHENG JIANG [1], (Member, IEEE), **YU ZHANG**[1], **JINSONG WU**[2,3], (Senior Member, IEEE), **WENJIANG FENG**[1], AND **YI JIN**[4]

[1] School of Microelectronics and Communication Engineering, Chongqing University, Chongqing 400044, China
[2] School of Artificial Intelligence, Guilin University of Electronic Technology, Guilin 541004, China
[3] Department of Electrical Engineering, Universidad de Chile, Santiago 8370451, Chile
[4] Xi'an Branch of China Academy of Space Technology, Xi'an 710100, China

Corresponding authors: Weiheng Jiang (whjiang@cqu.edu.cn) and Jinsong Wu (wujs@ieee.org)

ABSTRACT In this paper, we propose intelligent reflecting surfaces (IRS) assisted secure wireless communications with multi-input and multi-output antennas (IRS-MIMOME). The considered scenario is an access point (AP) equipped with multiple antennas communicates with a multi-antenna enabled legitimate user in the downlink at the present of an eavesdropper configured with multiple antennas. Particularly, the joint optimization of the transmit covariance matrix at the AP and the reflecting coefficients at the IRS to maximize the secrecy rate for the IRS-MIMOME system is investigated, with two different assumptions on the phase shifting capabilities at the IRS, i.e., the IRS has the continuous reflecting coefficients and the IRS has the discrete reflecting coefficients. For the former case, due to the non-convexity of the formulated problem, an alternating optimization (AO)-based algorithm is proposed, i.e., for given the reflecting coefficients at the IRS, the successive convex approximation (SCA)-based algorithm is used to solve the transmit covariance matrix optimization, while given the transmit covariance matrix at the AP, alternative optimization is used again in individually optimizing of each reflecting coefficient at the IRS with other fixed reflecting coefficients. For the individual reflecting coefficient optimization, the closed-form or an interval of the optimal solution is provided. Then, the proposed algorithm is extended to the discrete reflecting coefficient model at the IRS. Finally, some numerical simulations have been done to demonstrate that the proposed algorithm outperforms other benchmark schemes.

INDEX TERMS Alternating optimization (AO), intelligent reflecting surface (IRS), multiple-input multiple-output (MIMO), secrecy rate, successive convex approximation (SCA).

I. INTRODUCTION

Due to the broadcast nature of the wireless media, wireless communications are vulnerable to eavesdropping. In order to provide the wireless communications with sound and solid security, physical layer security based technologies, such as the artificial noise (AN), cooperative jamming (CJ) and friendly jamming, have been studied for the recent years [1], [2]. However, these techniques only focus on the

The associate editor coordinating the review of this manuscript and approving it for publication was Longxiang Gao.

signal processing at the transceiver to adaptive the changes of the wireless environments, but cannot eliminate the negative effects caused by the uncontrollable electromagnetic wave propagation environments [3], [4]. Meanwhile, recently, a new technology following the development of the Micro-Electro-Mechanical Systems (MEMS) named as intelligent reflecting surfaces (IRS) has been proposed, which can reconfigure and achieve a smart wireless propagation environment via software-controlled reflection. In addition, it has great potential in reducing the cost and the complexity and as well as energy consumption of the future 5G technologies such as

massive MIMO with excessive antennas [3]–[6], and also can support the development of the sustainable and green wireless networks in the coming years.

One the one hand, for the IRS assisted wireless communications, in [7], the problem of jointly optimizing the access point (AP) active beamforming and IRS passive beamforming with AP transmission power constraint to maximize the received signal power for one pair of transceivers was discussed. Based on the semidefinite relaxation and the alternate optimization, both the centralized algorithm and distributed algorithm were proposed therein. The work [8] extended the previous work to the multi-users scenario but with the individual signal-to-noise ratio (SNR) constraints, where the joint optimization of the AP active beamforming and IRS passive beamforming was discussed to minimize the total AP transmission power, and two suboptimal algorithms with different performance-complexity tradeoff were presented. Huang *et al.* considered the IRS-based multiple-input single-output (MISO) downlink multi-user communications for an outdoor environment, where [9] studied optimizing the base station (BS) transmission power and IRS phase shift with BS transmission power constraint and user signal-to-interference-and-noise-ratio (SINR) constraint to maximize sum system rate. Since the formulated resource allocation problem is non-convex, Majorization-Minimization (MM) and alternating optimization (AO) was jointly used, and the convergence of this algorithm was analyzed. Different from the continuous phase shift assumption of the IRS reflecting elements in existing studies, [10] considered that each IRS reflecting element can only achieve discrete phase shift and the joint optimization of the multi-antenna AP beamforming and IRS discrete phase shift was discussed under the same scenario as [7]. Then the performance loss caused by the IRS discrete phase shift was quantitatively analyzed via comparing with the IRS continuous phase shift. It is surprised that, the results have shown that as the number of IRS reflecting elements approaches infinity, the system can obtain the same square power gain as IRS with continuous phase shift, even based on 1-bit discrete phase shift. Furthermore, [11] and [12] discussed the joint AP power allocation and IRS phase-shift optimization to maximize system energy and spectrum efficiency, where the user has a minimum transmission rate constraint and the AP has a total transmit power constraint. Due to the presented problem is non-convex, the gradient descent based AP power allocation algorithm and fractional programming (FP) based IRS phase shift algorithm were proposed therein. For the IRS assisted wireless communication system, Han *et al.* [13] analyzed and obtained a compact approximation of system ergodic capacity and then, based on statistical channel information and approximate traversal capacity, the optimal IRS phase shift was proved. The authors also derived the required quantized bits of the IRS discrete phase shift system to obtain an acceptable ergodic capacity degradation. In [14], a new IRS hardware architecture was presented and then, based on compressed sensing and deep learning, two reflection beamforming methods were proposed with

different algorithm complexity and channel estimation training overhead. Similar to [14], Huang *et al.* [15] proposed a deep learning based algorithm to maximize the received signal strength for IRS-assisted indoor wireless communication environment. Some recently studies about the IRS assisted wireless communications could be found in [16]–[19], and they were focused on the IRS assisted millimeter band or non-orthogonal multiple access (NOMA) based wireless communications.

On the other hand, for the IRS assisted secure wireless communications, in [20], the authors studied the problem in jointly optimizing the beamforming at the transmitter and the IRS phase shifts to maximize the system secrecy rate, based on the block coordinate descent (BCD) and the MM techniques, two suboptimal algorithms were proposed to solve the resulted non-convex optimization problem for small- and large-scale IRS, respectively. In [21], Chen and Liang studied the minimum-secrecy-rate maximizing problem for a downlink MISO broadcast system, based on the AO and the path-following (PF) algorithm, an iterative algorithm was proposed for the joint optimization problem. In addition, the authors also extended the proposed approach to the case with discrete reflecting coefficients at the IRS. To maximize the MISO system secrecy rate subject to the source transmit power constraint and the unit modulus constraints imposed on the phase shifts at the IRS, [22] proposed an AO algorithm for the scenario that the eavesdropper is configured with single antenna, then the study was extended to the scenario where the eavesdropper is equipped with multiple antennas. Reference [23] investigated the secure transmission framework with an IRS to minimize the system energy consumption in cases of rank-one and full-rank AP-IRS links. In particular, since the beamforming vector and phase shift design are independent in the rank-one channel model, thus a closed-form expression of beamforming vector was derived. However, since beamforming and phase shift depend on each other in the full-rank model, then an eigenvalue-based algorithm for conventional wiretap channel was used to obtain beamforming vector. Different from [20]–[24] considered the scenario that the eavesdropping channel is stronger than the legitimate channel and they are also highly correlated in space, then to maximize the secrecy rate of the legitimate communication link, an algorithm based on the AO and semidefinite relaxation was proposed. Moreover, in [25] and [26], for the IRS assisted MISO secure communications with AN transmission at the transmitter, an alternate optimization algorithm to jointly optimize active beamforming, AN interference vector and reflection beamforming with the goal of maximizing system secrecy rate was presented. The difference between these two papers is that, [25] focused on the scenario with a single legitimate user and multiple eavesdroppers, while [26] considered the scenario with multiple legitimate users but single eavesdropper.

Although lots of research works have been done for the IRS assisted secure communications, they all have assumed that the legitimate receiver is equipped with only one

antenna [20]–[26]. However, in order to further improve the communication performance of the mobile users in the next generation wireless local networks (WLANs) such as the IEEE 802.11ax, or the fifth generation (5G) mobile communication networks, multi-antenna enabled mobile device designs have been widely adopted in the current mobile terminals, such as the Phones, laptops and the tablets. Therefore, it is necessary to study the IRS assisted secure communications with multiple-transmit and multiple-receive antennas enabled networks. In this paper, IRS assisted secure communications with multiple-transmit and multiple-receive antennas are studied, where, an AP equipped with multiple antennas has the secure communications demands with a multiple-antennas enabled legitimate user in the downlink at the present of an eavesdropper configured with multiple antennas, referring to it as the IRS assisted multi-input, multi-output, multi-eavesdropper (IRS-MIMOME) system. Particularly, we discuss the joint optimization of the transmit covariance matrix at the AP and the reflecting coefficients at the IRS to maximize the secrecy rate for the IRS-MIMOME system, with two different assumptions on the phase shifting capabilities at the IRS, i.e., the IRS has the continuous reflecting coefficients and the IRS has the discrete reflecting coefficients. For the former case, due to the non-convexity of the formulated problem, an AO based algorithm is proposed, i.e., for given the reflecting coefficients at the IRS, the successive convex approximation (SCA)-based algorithm is used to solve the transmit covariance matrix optimization, while given the transmit covariance matrix at the AP, alternative optimization is used again in the individually optimizing of each reflecting coefficient at the IRS with fixing the other reflecting coefficients. For the individual reflecting coefficient optimization, the closed-form or an interval of the optimal solution is provided. Then, the overall algorithm was extended to the discrete reflecting coefficient model at the IRS. Finally, some numerical simulations have been done to demonstrate the performance of the proposed algorithms.

The rest parts of this paper are organized as follows. In Section II, the system model and the considered optimization problem are presented. In Section III, we discuss and solve the formulated optimization problem, and an AO based algorithm is proposed. The simulation results are presented in Section IV and then we conclude this paper.

Notation: We use uppercase boldface letters for matrices and lowercase boldface letters for vectors. $(\bullet)^T$, $(\bullet)^*$, and $(\bullet)^H$ denote the transpose, conjugate, and conjugate transpose, respectively. $Tr(\bullet)$ and $\mathbb{E}\{\bullet\}$ stand for the trace of a matrix and the statistical expectation for random variables, respectively. $\mathbf{A} \succeq 0$ and $\mathbf{A} \succ 0$ indicate that $\mathbf{A}$ are positive semidefinite and positive definite matrix. $\mathbf{I}$ and $(\bullet)^{-1}$ denote the identity matrix with appropriate size and the inverse of a matrix, respectively. $| \bullet |$, $arg(\bullet)$ and $\Re\{\bullet\}$ stand for the absolute value, the argument and the real part of a complex number, respectively, whereas $\det(\mathbf{A})$ denotes the determinant of $\mathbf{A}$. The notation $diag(\bullet)$ represents a diagonal matrix where

the diagonal elements are from a vector, and $[\bullet]^+$ represents $\max(0, \bullet)$.

II. SYSTEM MODEL AND THE PROBLEM

In this section, firstly, we present the system model of the IRS assisted secure communications with multiple antennas at both the legitimate transceiver and the eavesdropper, referring to it as the IRS-MIMOME system. Then, we illustrate the IRS reflecting model and signal model for our considered system. Finally, we formulate the discussed optimization problem.

A. SYSTEM MODEL

Consider the IRS assisted MIMOME system, as shown in Fig. 1, where an AP equipped with N_T antennas serves a legitimate user at the present of an eavesdropper. Both the legitimate user and the eavesdropper are equipped with multi-antenna and the number of the antennas at these two users are N_R and N_E, respectively. In addition, an IRS composed of M passive elements is installed on a surrounding wall to assist the secure communications between the AP and the legitimate user. The IRS has a smart controller, who has the capability of dynamically adjusting the phase shift of each reflecting element based on the propagation environment learned through periodic sensing [7]. In particular, the IRS controller coordinates the switching between two working modes, i.e., receiving mode for environment sensing (e.g., channel state information (CSI) estimation) and reflecting mode for scattering the incident signals from the AP [27].
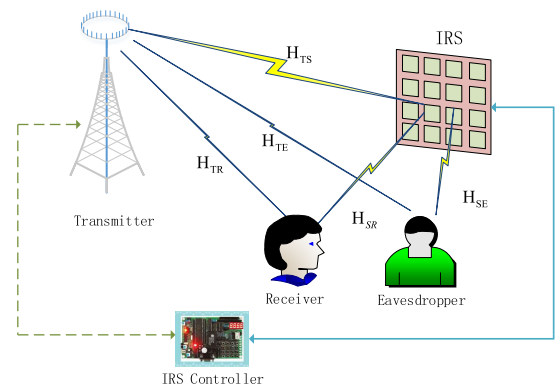

FIGURE 1. System model.

B. IRS REFLECTING COEFFICIENT MODEL

Following [7], the phase shift matrix of the IRS can be defined as $\Theta = diag(\boldsymbol{\theta}) \in \mathbb{C}^{M \times M}$, where $\boldsymbol{\theta} = [\theta_1, \theta_2, \cdots, \theta_M]^T \in \mathbb{C}^{M \times 1}$ and $\theta_m \in \boldsymbol{\Phi}$ for $1 \leq m \leq M$, and $diag(\bullet)$ denotes a diagonal matrix whose diagonal elements are given by the corresponding vector and $\boldsymbol{\Phi}$ denotes the set of reflecting coefficients of the IRS. In this paper, two different sets of reflecting coefficients are considered as below.

1) CONTINUOUS REFLECTING COEFFICIENTS

That is, the reflecting coefficient with the constant amplitude and continuous phase shift is characterized as

$$\boldsymbol{\Phi}_1 = \left\{ \theta_n \,\middle|\, \theta_n = e^{j\varphi_n}, \varphi_n \in [0, 2\pi) \right\}. \qquad (1)$$

2) DISCRETE REFLECTING COEFFICIENTS

In this model, the reflecting coefficient has constant amplitude but discrete phase shift and is defined as

$$\boldsymbol{\Phi}_2 = \left\{ \theta_n \left| \theta_n = e^{j\varphi_n}, \varphi_n \in \left\{ 0, \frac{2\pi}{Q}, \ldots, \frac{2\pi(Q-1)}{Q} \right\} \right. \right\}, \quad (2)$$

where Q is the number of quantized reflection coefficient values of the element of the IRS.

Note that, due to the limitations of the hardware, the realization of the continuous reflecting model $\boldsymbol{\Phi}_1$ is difficult or even impossible [21]. Therefore, the discrete model $\boldsymbol{\Phi}_2$ is more practical from the perspective of application. However, the continuous reflecting model is still discussed herein for the obtained performance can be regarded as the upper bound of the system. Furthermore, our algorithm for the discrete model is based on the algorithm of the continuous model.

C. SIGNAL MODEL

For our considered system, as [7] and [8], the signals that are reflected by the IRS multi-times are ignored due to significant path loss. Moreover, to characterize the performance limit of the considered IRS-assisted secure communication system, the quasi-static flat-fading channel model is adopted herein and all the CSI are perfectly known at the AP[1] [28], [29]. Therefore, combined with IRS reflecting coefficient model, the signals received at the legitimate user and the eavesdropper can be expressed as

$$\boldsymbol{y}_R = \mathbf{H}_{TR}\boldsymbol{x} + \mathbf{H}_{SR}\boldsymbol{\Theta}\mathbf{H}_{TS}\boldsymbol{x} + \boldsymbol{n}_R = \mathbf{G}_{TR}(\boldsymbol{\Theta})\boldsymbol{x} + \boldsymbol{n}_R, \quad (3)$$

$$\boldsymbol{y}_E = \mathbf{H}_{TE}\boldsymbol{x} + \mathbf{H}_{SE}\boldsymbol{\Theta}\mathbf{H}_{TS}\boldsymbol{x} + \boldsymbol{n}_E = \mathbf{G}_{TE}(\boldsymbol{\Theta})\boldsymbol{x} + \boldsymbol{n}_E, \quad (4)$$

where $\mathbf{H}_{TR} \in \mathbb{C}^{N_R \times N_T}$ and $\mathbf{H}_{TE} \in \mathbb{C}^{N_E \times N_T}$ represent the complex baseband channels from AP to the legitimate user and the eavesdropper, respectively, $\mathbf{H}_{SR} \in \mathbb{C}^{N_R \times M}$ and $\mathbf{H}_{SE} \in \mathbb{C}^{N_E \times M}$ denote the complex baseband channels from the IRS to the legitimate user and the eavesdropper, respectively, and $\mathbf{H}_{TS} \in \mathbb{C}^{M \times N_T}$ defines the complex baseband channel from AP to the IRS. $\mathbf{G}_{TR}(\boldsymbol{\Theta}) = \mathbf{H}_{TR} + \mathbf{H}_{SR}\boldsymbol{\Theta}\mathbf{H}_{TS}$ and $\mathbf{G}_{TE}(\boldsymbol{\Theta}) = \mathbf{H}_{TE} + \mathbf{H}_{SE}\boldsymbol{\Theta}\mathbf{H}_{TS}$ are used to characterize the equivalent channel from AP to the legitimate user and the eavesdropper, respectively. $\boldsymbol{n}_R \sim CN\left(0, \sigma_R^2\mathbf{I}_{N_R}\right)$ and $\boldsymbol{n}_E \sim CN\left(0, \sigma_E^2\mathbf{I}_{N_E}\right)$ denote the independent circularly symmetric complex Gaussian (CSCG) noise vectors at the legitimate user and the eavesdropper, respectively. In which, σ_R^2 and σ_E^2 denote the average noise power at the legitimate user and the eavesdropper, respectively. $\mathbf{I}_{N_R}$ and $\mathbf{I}_{N_E}$ represent the identity matrix with $N_R \times N_R$ and $N_E \times N_E$ dimensions, respectively.

For the above established IRS-MIMOME system, following [30], [31] and [32], we know that its achievable secrecy

rate is

$$R_{sec} = [R_R - R_E]^+, \quad (5)$$

where $[x]^+ = \max(0, x)$. And R_R and R_E represent the achievable transmission rates from AP to the legitimate user and from AP to the eavesdropper, respectively, and they are defined as follows,

$$R_R = \log_2 \det \left(\mathbf{I}_{N_R} + \frac{1}{\sigma_R^2} \mathbf{G}_{TR}(\boldsymbol{\Theta})\mathbf{Q}_s\mathbf{G}_{TR}^H(\boldsymbol{\Theta}) \right), \quad (6)$$

$$R_E = \log_2 \det \left(\mathbf{I}_{N_E} + \frac{1}{\sigma_E^2} \mathbf{G}_{TE}(\boldsymbol{\Theta})\mathbf{Q}_s\mathbf{G}_{TE}^H(\boldsymbol{\Theta}) \right), \quad (7)$$

where $\mathbf{Q}_s = \mathbb{E}\left\{\boldsymbol{x}\boldsymbol{x}^H\right\} \in \mathbb{C}^{N_T \times N_T}$ is the transmit signal covariance matrix at the AP and $\mathbf{Q}_s \succeq 0$. Hence, the achievable secrecy rate for the legitimate user is characterized by

$$R_{sec} = \left[\log_2 \det \left(\mathbf{I}_{N_R} + \frac{1}{\sigma_R^2} \mathbf{G}_{TR}(\boldsymbol{\Theta})\mathbf{Q}_s\mathbf{G}_{TR}^H(\boldsymbol{\Theta}) \right) \right.$$
$$\left. - \log_2 \det \left(\mathbf{I}_{N_E} + \frac{1}{\sigma_E^2} \mathbf{G}_{TE}(\boldsymbol{\Theta})\mathbf{Q}_s\mathbf{G}_{TE}^H(\boldsymbol{\Theta}) \right) \right]^+. \quad (8)$$

Note that dropping the operator $[\bullet]^+$ has no impact on the optimization of the secrecy rate, thus this operator is removed in the sequel analysis.

D. PROBLEM FORMULATION

As mentioned earlier, in this paper, we discuss the joint optimization of the transmit covariance matrix at the AP and the reflection coefficients at the IRS to maximize the system secrecy rate subjected to the transmit power constraint at the AP and the reflection coefficient constraint at the IRS. Thus we have the following optimization problem OP1,

$$\max_{\mathbf{Q}_s, \boldsymbol{\Theta}} R_{sec} = \log_2 \det \left(\mathbf{I}_{N_R} + \frac{1}{\sigma_R^2} \mathbf{G}_{TR}(\boldsymbol{\Theta})\mathbf{Q}_s\mathbf{G}_{TR}^H(\boldsymbol{\Theta}) \right)$$
$$- \log_2 \det \left(\mathbf{I}_{N_E} + \frac{1}{\sigma_E^2} \mathbf{G}_{TE}(\boldsymbol{\Theta})\mathbf{Q}_s\mathbf{G}_{TE}^H(\boldsymbol{\Theta}) \right)$$
$$s.t.\ C1 : Tr(\mathbf{Q}_s) \leq P_{\max}$$
$$C2 : \mathbf{Q}_s \succeq 0$$
$$C3 : \theta_m \in \boldsymbol{\Phi}_i, \quad m = 1, \ldots, M,\ i = 1, 2. \quad (9)$$

In which, C1 characterizes the total transmit power constraint at the AP, C2 defines the positive semi-definite constraint on transmit covariance matrix, and C3 represents the IRS reflecting coefficient model. It is obvious that OP1 is a non-convex nonlinear programming with non-convex objective function and the uni-modular constraint on each reflection coefficient θ_m, which makes it difficult to be solved. Therefore, in the sequel, we pursue the suboptimal approach to handle OP1.

---

[1]Due to the fact that the transceivers are equipped with multiple antennas and the number of the element on the IRS is large, therefore, to accurately estimate the channels is impossible, then it will induce system performance loss if naively treating the estimated channels as perfect ones. However, our work is still meaningful as it can be seen as the benchmark for the imperfect CSI case. In addition, how to extend our work to the scenario with imperfect CSI is an interesting problem and it is our future work.

III. ALTERNATING OPTIMIZATION BASED JOINT OPTIMIZATION ALGORITHM

In this section, a suboptimal algorithm is proposed to solve OP1. As aforementioned that, our formulated problem OP1 is a non-convex nonlinear programming. However, our analysis indicates that, given the reflecting coefficients at the IRS and by leveraging the SCA [33], a convex approach can be used to solve the transmit covariance matrix optimization at the AP, while for given the transmit covariance matrix at the AP, we can use the alternative optimization to find the suboptimal solution for the reflecting coefficients at the IRS. Based on that, we present an alternative suboptimal algorithm for OP1. In addition, we also discuss the extension of the algorithm to the case with discrete reflecting coefficients at the IRS at the end of this section.

A. OPTIMIZATION OF THE TRANSMIT COVARIANCE MATRIX

In this subsection, we discuss the transmit covariance matrix optimization at the AP for given the reflecting coefficients at the IRS. Hence, we have the following problem OP2,

$$\max_{\mathbf{Q}_s} R_{sec}(\mathbf{Q}_s) = R_R(\mathbf{Q}_s) - R_E(\mathbf{Q}_s)$$

$$= \log_2 \det\left(\mathbf{I}_{N_R} + \frac{1}{\sigma_R^2}\mathbf{G}_{TR}\mathbf{Q}_s\mathbf{G}_{TR}^H\right)$$

$$- \log_2 \det\left(\mathbf{I}_{N_E} + \frac{1}{\sigma_E^2}\mathbf{G}_{TE}\mathbf{Q}_s\mathbf{G}_{TE}^H\right),$$

$$s.t. \ C1 : Tr(\mathbf{Q}_s) \leq P_{\max},$$

$$C2 : \mathbf{Q}_s \succeq 0. \tag{10}$$

Herein, given the reflection coefficient matrix Θ at the IRS, $\mathbf{G}_{TR}(\Theta)$ and $\mathbf{G}_{TE}(\Theta)$ are simplistically denoted as $\mathbf{G}_{TR}$ and $\mathbf{G}_{TE}$, respectively. One may note that, now, the formulated problem OP2 is the secrecy rate maximization problem for the MIMOME system which has been discussed in [33], [34] and [35], and various algorithms have been proposed therein. In this paper, following [33], the SCA-based suboptimal algorithm is used to handle OP2. And the key point is to obtain a tight concave lower bound of $R_{sec}(\mathbf{Q}_s)$, which can be achieved by retaining the concave part $R_R(\mathbf{Q}_s)$ in (10) and linearizing the concave function $R_E(\mathbf{Q}_s)$ [36], [37]. That is, at $\tilde{\mathbf{Q}}_s$, we have the concave approximation of $R_{sec}(\mathbf{Q}_s)$ as follows,

$$R_{sec}(\mathbf{Q}_s) = \log_2 \det\left(\mathbf{I}_{N_R} + \frac{1}{\sigma_R^2}\mathbf{G}_{TR}\mathbf{Q}_s\mathbf{G}_{TR}^H\right)$$

$$- \log_2 \det\left(\mathbf{I}_{N_E} + \frac{1}{\sigma_E^2}\mathbf{G}_{TE}\mathbf{Q}_s\mathbf{G}_{TE}^H\right)$$

$$\simeq \log_2 \det\left(\mathbf{I}_{N_R} + \frac{1}{\sigma_R^2}\mathbf{G}_{TR}\mathbf{Q}_s\mathbf{G}_{TR}^H\right)$$

$$- \log_2 \det\left(\mathbf{I}_{N_E} + \frac{1}{\sigma_E^2}\mathbf{G}_{TE}\tilde{\mathbf{Q}}_s\mathbf{G}_{TE}^H\right)$$

$$- Tr\left[\frac{1}{ln2}\frac{1}{\sigma_E^2}\mathbf{W}_{E,\tilde{\mathbf{Q}}_s}^{-1}\mathbf{G}_{TE}\mathbf{Q}_s\mathbf{G}_{TE}^H\right]$$

$$+ Tr\left[\frac{1}{ln2}\frac{1}{\sigma_E^2}\mathbf{W}_{E,\tilde{\mathbf{Q}}_s}^{-1}\mathbf{G}_{TE}\tilde{\mathbf{Q}}_s\mathbf{G}_{TE}^H\right]$$

$$\triangleq \tilde{R}_{sec}\left(\mathbf{Q}_s \big| \tilde{\mathbf{Q}}_s\right), \tag{11}$$

where $\mathbf{W}_{E,\tilde{\mathbf{Q}}_s} = \mathbf{I}_{N_E} + \frac{1}{\sigma_E^2}\mathbf{G}_{TE}\tilde{\mathbf{Q}}_s\mathbf{G}_{TE}^H$. Based on the above approximation and given $\tilde{\mathbf{Q}}_s$, the problem OP2 can be transformed into the following formulation,

$$\max_{\mathbf{Q}_s} \tilde{R}_{sec}\left(\mathbf{Q}_s \big| \tilde{\mathbf{Q}}_s\right)$$

$$s.t. \ C1 : Tr(\mathbf{Q}_s) \leq P_{\max}$$

$$C2 : \mathbf{Q}_s \succeq 0. \tag{12}$$

Then this problem is convex and can be easily solved using standard interior-point methods [33], and the Lagrange dual problem of (12) is provided at Appendix A. To sum up, we have the SCA based suboptimal algorithm for OP2 which is summarized as the Algorithm 1 as below.

Algorithm 1 Optimize Transmit Covariance Matrix
S1: Initialize: $\tilde{\mathbf{Q}}_s \succeq 0$ and $\lambda = \lambda_0 > 0$;
S2: Repeat
S3: Repeat
a) Solve the problem in (33) with given $\tilde{\mathbf{Q}}_s$ and λ,
Obtain the optimal transmit covariance $\hat{\mathbf{Q}}_s$;
b) Update λ based on the subgradient method;
S4: Until the required accuracy;
S5: Update $\tilde{\mathbf{Q}}_s = \hat{\mathbf{Q}}_s$, and reset $\lambda = \lambda_0$;
S6: Until the required accuracy;
S7: Output $\hat{\mathbf{Q}}_s$.

To meet the transmission power constraint at the AP and the positive semi-definite constraint of the transmit covariance matrix $\mathbf{Q}_s$ at the beginning of the algorithm, we set $\tilde{\mathbf{Q}}_s = (P_{\max}/N_T)\mathbf{I}_{N_T}$.

B. OPTIMIZE THE IRS REFLECTING COEFFICIENTS

In this subsection, given the transmit covariance matrix $\mathbf{Q}_s$ at the AP, the optimization the reflecting coefficient matrix Θ at IRS with the continuous model is discussed. Particularly, we have the following problem OP3.

$$\max_{\Theta} R_{sec}(\Theta) = \log_2 \det\left(\mathbf{I}_{N_R} + \frac{1}{\sigma_R^2}\mathbf{G}_{TR}(\Theta)\mathbf{Q}_s\mathbf{G}_{TR}^H(\Theta)\right)$$

$$- \log_2 \det\left(\mathbf{I}_{N_E} + \frac{1}{\sigma_E^2}\mathbf{G}_{TE}(\Theta)\mathbf{Q}_s\mathbf{G}_{TE}^H(\Theta)\right)$$

$$s.t. \ \theta_m \in \mathbf{\Phi}_1, \quad m = 1, 2, \ldots, M \tag{13}$$

It is obvious that OP3 is a non-convex programming with both non-convex constraints and non-concave objective function, which makes it is difficult to be solved. However,

we prove that, given $\{\theta_i\}_{i=1,i\neq m}^{M}$, the formulated optimization problem with respect to θ_m can be solved with the closed-form optimal solution or to have an interval about the optimal solution. Therefore, the alternative optimization approach is used here again to solve OP3, i.e., we alternatively solve OP3 in variable θ_m with given $\theta_i, i = 1, \ldots, M, i \neq m$ until the procedure is converged. The details are illustrated as follows.

1) Objective function transformation: In order to use the alternative optimization approach to solve OP3, we should first make an objective function transformation for OP3. Note that, the relationship of the objective function with $\{\theta_m\}_{m=1}^{M}$ is rather implicit. Thus, we rewrite the objective function as an explicit function over $\theta_m, \forall m$. That is [38],

$$
\begin{aligned}
&R_{sec}(\Theta)\\
&= \log_2 \det\left(\mathbf{I}_{N_R} + \frac{1}{\sigma_R^2}\overline{\mathbf{H}}_{TR}\overline{\mathbf{H}}_{TR}^{H}\right.\\
&\quad + \frac{1}{\sigma_R^2}\sum_{i=1}^{M} \boldsymbol{h}_{SR,i}\overline{\boldsymbol{h}}_{TS,i}^{H}\overline{\boldsymbol{h}}_{TS,i}\boldsymbol{h}_{SR,i}^{H}\\
&\quad + \frac{1}{\sigma_R^2}\sum_{i=1}^{M}\sum_{j=1,j\neq i}^{M}\theta_i\theta_j^*\boldsymbol{h}_{SR,i}\overline{\boldsymbol{h}}_{TS,i}^{H}\overline{\boldsymbol{h}}_{TS,j}\boldsymbol{h}_{SR,j}^{H}\\
&\quad \left.+ \frac{1}{\sigma_R^2}\sum_{i=1}^{M}\left(\overline{\mathbf{H}}_{TR}\theta_i^*\overline{\boldsymbol{h}}_{TS,i}\boldsymbol{h}_{SR,i}^{H} + \theta_i\boldsymbol{h}_{SR,i}\overline{\boldsymbol{h}}_{TS,i}^{H}\overline{\mathbf{H}}_{TR}^{H}\right)\right)\\
&\quad - \log_2 \det\left(\mathbf{I}_{N_E} + \frac{1}{\sigma_E^2}\overline{\mathbf{H}}_{TE}\overline{\mathbf{H}}_{TE}^{H}\right.\\
&\quad + \frac{1}{\sigma_E^2}\sum_{i=1}^{M} \boldsymbol{h}_{SE,i}\overline{\boldsymbol{h}}_{TS,i}^{H}\overline{\boldsymbol{h}}_{TS,i}\boldsymbol{h}_{SE,i}^{H}\\
&\quad + \frac{1}{\sigma_E^2}\sum_{i=1}^{M}\sum_{j=1,j\neq i}^{M}\theta_i\theta_j^*\boldsymbol{h}_{SE,i}\overline{\boldsymbol{h}}_{TS,i}^{H}\overline{\boldsymbol{h}}_{TS,j}\boldsymbol{h}_{SE,j}^{H}\\
&\quad \left.+ \frac{1}{\sigma_E^2}\sum_{i=1}^{M}\left(\overline{\mathbf{H}}_{TE}\theta_i^*\overline{\boldsymbol{h}}_{TS,i}\boldsymbol{h}_{SE,i}^{H} + \theta_i\boldsymbol{h}_{SE,i}\overline{\boldsymbol{h}}_{TS,i}^{H}\overline{\mathbf{H}}_{TE}^{H}\right)\right)
\end{aligned}
\tag{14}
$$

Herein, let $\mathbf{Q}_s = \mathbf{U}_Q\Sigma_Q\mathbf{U}_Q^{H}$ as the eigenvalue decomposition (EVD) of $\mathbf{Q}_s \succeq 0$, $\mathbf{U}_Q \in \mathbb{C}^{N_T \times N_T}$ and $\Sigma_Q \in \mathbb{C}^{N_T \times N_T}$ are unitary matrix and diagonal matrix, respectively, and all the diagonal elements in Σ_Q are non-negative real numbers. Also, in (14), we define $\mathbf{H}_{SR} = [\boldsymbol{h}_{SR,1}, \ldots, \boldsymbol{h}_{SR,M}]$, $\mathbf{H}_{SE} = [\boldsymbol{h}_{SE,1}, \ldots, \boldsymbol{h}_{SE,M}]$, $\overline{\mathbf{H}}_{TS} = \mathbf{H}_{TS}\mathbf{U}_Q\Sigma_Q^{1/2} = [\overline{\boldsymbol{h}}_{TS,1}, \ldots, \overline{\boldsymbol{h}}_{TR,M}]^{H}$, $\overline{\mathbf{H}}_{TR} = \mathbf{H}_{TR}\mathbf{U}_Q\Sigma_Q^{1/2} \in \mathbb{C}^{N_R \times N_T}$, $\overline{\mathbf{H}}_{TE} = \mathbf{H}_{TE}\mathbf{U}_Q\Sigma_Q^{1/2} \in \mathbb{C}^{N_E \times N_T}$, and $\boldsymbol{h}_{SR,m} \in \mathbb{C}^{N_R \times 1}$, $\boldsymbol{h}_{SE,m} \in \mathbb{C}^{N_E \times 1}$, $\overline{\boldsymbol{h}}_{TS,m} \in \mathbb{C}^{N_T \times 1}$, $m = 1, 2, \ldots M$. Now, R_{sec} is represented in an explicit form of the reflection coefficients $\{\theta_m\}_{m=1}^{M}$. Therefore, given $\mathbf{Q}_s$ and $\{\theta_i\}_{i=1,i\neq m}^{M}$, R_{sec} can be rewritten as a function of θ_m as,

$$
R_{sec}(\theta_m) = \log_2 \det\left(\mathbf{A}_{R,m} + \theta_m\mathbf{B}_{R,m} + \theta_m^*\mathbf{B}_{R,m}^{H}\right) - \log_2 \det
$$
$$
\times \left(\mathbf{A}_{E,m} + \theta_m\mathbf{B}_{E,m} + \theta_m^*\mathbf{B}_{E,m}^{H}\right), \quad \forall m, \tag{15}
$$

where,

$$
\mathbf{A}_{R,m} = \mathbf{I}_{N_R} + \frac{1}{\sigma_R^2}\hat{\mathbf{H}}_R\hat{\mathbf{H}}_R^{H} + \frac{1}{\sigma_R^2}\tilde{\mathbf{H}}_R\tilde{\mathbf{H}}_R^{H}, \quad \forall m,
$$

$$
\mathbf{B}_{R,m} = \frac{1}{\sigma_R^2}\tilde{\mathbf{H}}_R\hat{\mathbf{H}}_R^{H}, \quad \forall m,
$$

$$
\mathbf{A}_{E,m} = \mathbf{I}_{N_E} + \frac{1}{\sigma_E^2}\hat{\mathbf{H}}_E\hat{\mathbf{H}}_E^{H} + \frac{1}{\sigma_E^2}\tilde{\mathbf{H}}_E\tilde{\mathbf{H}}_E^{H}, \quad \forall m,
$$

$$
\mathbf{B}_{E,m} = \frac{1}{\sigma_E^2}\tilde{\mathbf{H}}_E\hat{\mathbf{H}}_E^{H}, \quad \forall m. \tag{16}
$$

We denote $\hat{\mathbf{H}}_R = \overline{\mathbf{H}}_{TR} + \sum_{i=1,i\neq m}^{M}\theta_i\boldsymbol{h}_{SR,i}\overline{\boldsymbol{h}}_{TS,i}^{H}$, $\hat{\mathbf{H}}_E = \overline{\mathbf{H}}_{TE} + \sum_{i=1,i\neq m}^{M}\theta_i\boldsymbol{h}_{SE,i}\overline{\boldsymbol{h}}_{TS,i}^{H}$, $\tilde{\mathbf{H}}_R = \boldsymbol{h}_{SR,m}\overline{\boldsymbol{h}}_{TS,m}^{H}$ and $\tilde{\mathbf{H}}_E = \boldsymbol{h}_{SE,m}\overline{\boldsymbol{h}}_{TS,m}^{H}$. Since both $\mathbf{A}_{R,m}$ and $\mathbf{A}_{E,m}$ are the sum of identity matrix and the two positive semi-definite matrixes, thus we have $\mathbf{A}_{R,m} \succ 0$, $\mathbf{A}_{E,m} \succ 0$, $rank\left(\mathbf{A}_{R,m}\right) = N_R$ and $rank\left(\mathbf{A}_{E,m}\right) = N_E$. Moreover, for $\mathbf{B}_{R,m}$ and $\mathbf{B}_{E,m}$ we have $rank\left(\mathbf{B}_{R,m}\right) \leq rank\left(\boldsymbol{h}_{SR,m}\overline{\boldsymbol{h}}_{TS,m}^{H}\right) \leq 1$ and $rank\left(\mathbf{B}_{E,m}\right) \leq rank\left(\boldsymbol{h}_{SE,m}\overline{\boldsymbol{h}}_{TS,m}^{H}\right) \leq 1$, respectively. Therefore, $R_{sec}(\theta_m)$ can be rewritten as

$$
\begin{aligned}
R_{sec}(\theta_m) &= \log_2 \det\left(\mathbf{I}_{N_R} + \theta_m\mathbf{J}_R + \theta_m^*\mathbf{J}_R^{H}\right)\\
&\quad - \log_2 \det\left(\mathbf{I}_{N_E} + \theta_m\mathbf{J}_E + \theta_m^*\mathbf{J}_E^{H}\right)\\
&\quad + \log_2 \det\left(\mathbf{A}_{R,m}\right) - \log_2 \det\left(\mathbf{A}_{E,m}\right)\\
&= \overline{R}_{sec}(\theta_m) + \log_2 \det\left(\mathbf{A}_{R,m}\right)\\
&\quad - \log_2 \det\left(\mathbf{A}_{E,m}\right)
\end{aligned}
\tag{17}
$$

Herein, $\mathbf{J}_R = \mathbf{A}_{R,m}^{-1}\mathbf{B}_{R,m}$ and $\mathbf{J}_E = \mathbf{A}_{E,m}^{-1}\mathbf{B}_{E,m}$. Hence, the maximization of R_{sec} is equivalent to maximize the $\overline{R}_{sec}$, namely,

$$
\begin{aligned}
\overline{R}_{sec}(\theta_m) &= \log_2 \det\left(\mathbf{I}_{N_R} + \theta_m\mathbf{J}_R + \theta_m^*\mathbf{J}_R^{H}\right)\\
&\quad - \log_2 \det\left(\mathbf{I}_{N_E} + \theta_m\mathbf{J}_E + \theta_m^*\mathbf{J}_E^{H}\right)\\
&= \overline{R}_R(\theta_m) - \overline{R}_E(\theta_m)
\end{aligned}
$$
$$
s.t. \ |\theta_m| = 1 \tag{18}
$$

Herein, $\overline{R}_R(\theta_m) = \log_2 \det(\mathbf{I}_{N_R} + \theta_m\mathbf{J}_R + \theta_m^*\mathbf{J}_R^{H})$ and $\overline{R}_E(\theta_m) = \log_2 \det(\mathbf{I}_{N_E} + \theta_m\mathbf{J}_E + \theta_m^*\mathbf{J}_E^{H})$. In addition, due to both $\mathbf{A}_{R,m}$ and $\mathbf{A}_{E,m}$ are full-rank, we have $rank(\mathbf{J}_R) = rank\left(\mathbf{B}_{R,m}\right) \leq 1$ and $rank(\mathbf{J}_E) = rank\left(\mathbf{B}_{E,m}\right) \leq 1$.

2) Deriving the tractable expressions for $\overline{R}_R(\theta_m)$ and $\overline{R}_E(\theta_m)$ [38]: Following the above, herein, according to the value of $rank(\mathbf{J}_R)$ (or $rank(\mathbf{J}_E)$), i.e., $rank(\mathbf{J}_R) = 1$ ($rank(\mathbf{J}_E) = 1$) or $rank(\mathbf{J}_R) = 0$ ($rank(\mathbf{J}_E) = 0$), we separately derive the tractable expressions of $\overline{R}_R(\theta_m)$ and $\overline{R}_E(\theta_m)$ which are then used to analyze the corresponding optimal solution of θ_m.

Case $rank(\mathbf{J}_R) = 1$: At first, we present a lemma as below.

Lemma 1 ([38]): $\mathbf{J}_R$ is diagonalizable if and only if $Tr(\mathbf{J}_R) \neq 0$.

Based on the Lemma 1, then we can derive the expression of $\overline{R}_R(\theta_m)$ under $Tr(\mathbf{J}_R) = 0$ and $Tr(\mathbf{J}_R) \neq 0$, separately.

If $Tr(\mathbf{J}_R) = 0$, namely, $\mathbf{J}_R$ is non-diagonalizable, $\mathbf{J}_R = \mathbf{u}_{R,m}\mathbf{v}_{R,m}^H$ with $\mathbf{u}_{R,m}, \mathbf{v}_{R,m} \in \mathbb{C}^{N_R \times 1}$ and $\mathbf{v}_{R,m}^H \mathbf{u}_{R,m} = \mathbf{u}_{R,m}^H \mathbf{v}_{R,m} = Tr(\mathbf{J}_R) = 0$ due to $rank(\mathbf{J}_R) = 1$. Hence, the expression of $\overline{R}_R(\theta_m)$ can be transformed into

$$
\begin{aligned}
\overline{R}_R(\theta_m) &= \log_2 \det\left(\mathbf{I}_{N_R} - \mathbf{A}_{R,m}^{-1}\mathbf{v}_{R,m}\mathbf{u}_{R,m}^H\mathbf{A}_{R,m}\mathbf{u}_{R,m}\mathbf{v}_{R,m}^H\right) \\
&= \log_2 \det\left(\mathbf{I}_{N_R} - \mathbf{A}_{R,m}^{-1}\mathbf{J}_R^H\mathbf{A}_{R,m}\mathbf{J}_R\right) \\
&= \log_2 \det\left(\mathbf{I}_{N_R} - \mathbf{A}_{R,m}^{-1}\mathbf{B}_{R,m}^H\mathbf{J}_R\right),
\end{aligned}
$$

in which, the last equation is hold with $\mathbf{A}_{R,m}^{-1} = \left(\mathbf{A}_{R,m}^{-1}\right)^H$ for $\mathbf{A}_{R,m} \succ 0$.

If $Tr(\mathbf{J}_R) \neq 0$, the EVD of $\mathbf{J}_R$ can be expressed as $\mathbf{J}_R = \mathbf{U}_{R,m}\Sigma_{R,m}\mathbf{U}_{R,m}^{-1}$, where, $\mathbf{U}_{R,m} \in \mathbb{C}^{N_R \times N_R}$ and $\Sigma_{R,m} = diag\{\lambda_{R,m}, 0, \ldots, 0\}$ with $\lambda_{R,m}$ denoting the sole non-zero eigenvalue of $\mathbf{J}_R$. Set $\mathbf{V}_{R,m} = \mathbf{U}_{R,m}^H\mathbf{A}_{R,m}\mathbf{U}_{R,m}$ and it is a Hermitian matrix with $\mathbf{V}_{R,m} = \mathbf{V}_{R,m}^H$. Let $\mathbf{v}_{R,m} \in \mathbb{C}^{N_R \times 1}$ and $\overline{\mathbf{v}}_{R,m}^T \in \mathbb{C}^{1 \times N_R}$ denote the first column of $\mathbf{V}_{R,m}^{-1}$ and the first row of $\mathbf{V}_{R,m}$. Note that it follows that $\overline{\mathbf{v}}_{R,m}^T\mathbf{v}_{R,m} = 1$; moreover, let $v_{R,m1}$ and $\overline{v}_{R,m1}$ denote the first element in $\mathbf{v}_{R,m}$ and $\overline{\mathbf{v}}_{R,m}^T$, respectively, we have $\overline{v}_{R,m1}v_{R,m1} \in \mathbb{R}$ since both $\mathbf{V}_{R,m}$ and $\mathbf{V}_{R,m}^{-1}$ are Hermitian matrices. Hence, $\overline{R}_R(\theta_m)$ can be further simplified as [38],

$$
\begin{aligned}
\overline{R}_R(\theta_m) = \log_2 \Big(1 + |\lambda_{R,m}|^2\left(1 - \overline{v}_{R,m1}v_{R,m1}\right) \\
+ 2\Re\{\theta_m\lambda_{R,m}\}\Big) \quad (19)
\end{aligned}
$$

Case rank$(\mathbf{J}_E) = 1$: Similarly, **if** $Tr(\mathbf{J}_E) = 0$, we have

$$
\overline{R}_E(\theta_m) = \log_2 \det\left(\mathbf{I}_{N_E} - \mathbf{A}_{E,m}^{-1}\mathbf{B}_{E,m}^H\mathbf{J}_E\right) \quad (20)
$$

And if $Tr(\mathbf{J}_E) \neq 0$, the EVD of $\mathbf{J}_E$ can be expressed as $\mathbf{J}_E = \mathbf{U}_{E,m}\Sigma_{E,m}\mathbf{U}_{E,m}^{-1}$, where, $\mathbf{U}_{E,m} \in \mathbb{C}^{N_E \times N_E}$ and $\Sigma_{E,m} = diag\{\lambda_{E,m}, 0, \ldots, 0\}$ with $\lambda_{E,m}$ denoting the sole non-zero eigenvalue of $\mathbf{J}_E$. Set $\mathbf{V}_{E,m} = \mathbf{U}_{E,m}^H\mathbf{A}_{E,m}\mathbf{U}_{E,m}$, let $\mathbf{v}_{E,m} \in \mathbb{C}^{N_E \times 1}$ and $\overline{\mathbf{v}}_{E,m}^T \in \mathbb{C}^{1 \times N_E}$ denote the first column of $\mathbf{V}_{E,m}^{-1}$ and the first row of $\mathbf{V}_{E,m}$ and let $v_{E,m1}$ and $\overline{v}_{E,m1}$ denote the first element in $\mathbf{v}_{E,m}$ and $\overline{\mathbf{v}}_{E,m}^T$, respectively. Hence, $\overline{R}_E(\theta_m)$ can be further simplified as,

$$
\begin{aligned}
\overline{R}_E(\theta_m) = \log_2 \Big(1 + |\lambda_{E,m}|^2\left(1 - \overline{v}_{E,m1}v_{E,m1}\right) \\
+ 2\Re\{\theta_m\lambda_{E,m}\}\Big) \quad (21)
\end{aligned}
$$

Case rank$(\mathbf{J}_R) = 0$ *or rank*$(\mathbf{J}_E) = 0$: In fact, if $rank(\mathbf{J}_R) = 0$, we always have $\mathbf{J}_R = \mathbf{0}$ and $\mathbf{J}_R = \mathbf{u}_{R,m}\mathbf{v}_{R,m}^H$ with $\mathbf{u}_{R,m} = \mathbf{v}_{R,m} = 0$, which is equivalent to the case $Tr(\mathbf{J}_R) = 0$ under $rank(\mathbf{J}_R) = 1$. Similarly, the case $rank(\mathbf{J}_E) = 0$ is equivalent to the case $Tr(\mathbf{J}_E) = 0$ under $rank(\mathbf{J}_E) = 1$. Therefore, no matter whether $rank(\mathbf{J}_R) = 1$ or $rank(\mathbf{J}_R) = 0$ ($rank(\mathbf{J}_E) = 1$ or $rank(\mathbf{J}_E) = 0$), a tractable expression of $\overline{R}_R(\theta_m)$ ($\overline{R}_E(\theta_m)$) only depends on the value of $Tr(\mathbf{J}_R)$ ($Tr(\mathbf{J}_E)$), i.e., $Tr(\mathbf{J}_R) = 0$ or $Tr(\mathbf{J}_R) \neq 0$ ($Tr(\mathbf{J}_E) = 0$ or $Tr(\mathbf{J}_E) \neq 0$).

3) Solving problem (18): Based on the deriving of the tractable expressions for $\overline{R}_R(\theta_m)$ and $\overline{R}_E(\theta_m)$, we know that problem (18) should be discussed and solved by considering four different conditions, i.e., $Tr(\mathbf{J}_R) = 0$ and $Tr(\mathbf{J}_E) = 0$, $Tr(\mathbf{J}_R) \neq 0$ and $Tr(\mathbf{J}_E) = 0$, $Tr(\mathbf{J}_R) = 0$ and $Tr(\mathbf{J}_E) \neq 0$, and $Tr(\mathbf{J}_R) \neq 0$ and $Tr(\mathbf{J}_E) \neq 0$, as follows.

Case $Tr(\mathbf{J}_R) = Tr(\mathbf{J}_E) = 0$: Namely, both $\mathbf{J}_R$ and $\mathbf{J}_E$ are non-diagonalizable. In this case, $\overline{R}_{sec}(\theta_m)$ is defined as

$$
\begin{aligned}
\overline{R}_{sec}(\theta_m) = \log_2 \det\left(\mathbf{I}_{N_R} - \mathbf{A}_{R,m}^{-1}\mathbf{B}_{R,m}^H\mathbf{J}_R\right) \\
- \log_2 \det\left(\mathbf{I}_{N_E} - \mathbf{A}_{E,m}^{-1}\mathbf{B}_{E,m}^H\mathbf{J}_E\right). \quad (22)
\end{aligned}
$$

That is, $\overline{R}_{sec}(\theta_m)$ is independent of θ_m. Hence, we can directly obtain the optimal solution for (18) and it is characterized by the following proposition. Since the proof is simply thus it is omitted here for simplification.

Proposition 2: If $Tr(\mathbf{J}_R) = Tr(\mathbf{J}_E) = 0$, any θ_m with $|\theta_m| = 1$ is the optimal solution for (18) and the corresponding optimal value is

$$
\begin{aligned}
\hat{R}_{sec}(\theta_m) = \log_2 \det\left(\mathbf{A}_{R,m} - \mathbf{B}_{R,m}^H\mathbf{J}_R\right) \\
- \log_2 \det\left(\mathbf{A}_{E,m} - \mathbf{B}_{E,m}^H\mathbf{J}_E\right). \quad (23)
\end{aligned}
$$

Case $Tr(\mathbf{J}_R) \neq 0$ *and* $Tr(\mathbf{J}_E) = 0$: Namely, $\mathbf{J}_R$ is diagonalizable and $\mathbf{J}_E$ is non-diagonalizable. In this case, $\overline{R}_{sec}(\theta_m)$ is denoted as

$$
\begin{aligned}
\overline{R}_{sec}(\theta_m) = \log_2 \Big(1 + |\lambda_{R,m}|^2\left(1 - \overline{v}_{R,m1}v_{R,m1}\right) \\
+ 2\Re\{\theta_m\lambda_{R,m}\}\Big) \\
- \log_2 \det\left(\mathbf{I}_{N_E} - \mathbf{A}_{E,m}^{-1}\mathbf{B}_{E,m}^H\mathbf{J}_E\right). \quad (24)
\end{aligned}
$$

Now, for problem (18), maximizing $\overline{R}_{sec}(\theta_m)$ is equivalent to maximize $\Re\{\theta_m\lambda_{E,m}\}$ in (24) and the corresponding optimal solution can be characterized by the following Proposition 3.

Proposition 3: If $Tr(\mathbf{J}_R) \neq 0$ and $Tr(\mathbf{J}_E) = 0$, the optimal solution to (18) is

$$
\hat{\theta}_m = e^{-j\arg(\lambda_{R,m})},
$$

and the corresponding optimal value is

$$
\begin{aligned}
\hat{R}_{sec}(\theta_m) = \log_2 \Big(1 + |\lambda_{R,m}|^2\left(1 - \overline{v}_{R,m1}v_{R,m1}\right) \\
+ 2|\lambda_{R,m}|\Big) + \log_2 \det\left(\mathbf{A}_{R,m}\right) \\
- \log_2 \det\left(\mathbf{A}_{E,m} - \mathbf{B}_{E,m}^H\mathbf{J}_E\right).
\end{aligned}
$$

Proof: The proof is provided in Appendix B. ∎

Case $Tr(\mathbf{J}_R) = 0$ *and* $Tr(\mathbf{J}_E) \neq 0$: Namely, $\mathbf{J}_R$ is non-diagonalizable and $\mathbf{J}_E$ is diagonalizable, then $\overline{R}_{sec}(\theta_m)$ becomes

$$
\begin{aligned}
\overline{R}_{sec}(\theta_m) = \log_2 \det\left(\mathbf{I}_{N_R} - \mathbf{A}_{R,m}^{-1}\mathbf{B}_{R,m}^H\mathbf{J}_R\right) \\
- \log_2 \Big(1 + |\lambda_{E,m}|^2\left(1 - \overline{v}_{E,m1}v_{E,m1}\right) \\
+ 2\Re\{\theta_m\lambda_{E,m}\}\Big). \quad (25)
\end{aligned}
$$

Now, for problem (18), maximizing $\overline{R}_{sec}(\theta_m)$ is equivalent to minimize $\Re\{\theta_m \lambda_{E,m}\}$ in (25) and the corresponding optimal solution can be characterized by the following Proposition 4.

Proposition 4: If $Tr(\mathbf{J}_R) = 0$ and $Tr(\mathbf{J}_E) \neq 0$, the optimal solution for (18) is

$$\hat{\theta}_m = e^{j(\pi - \arg(\lambda_{E,m}))},$$

and the corresponding optimal value is

$$\hat{R}_{sec}(\theta_m) = \log_2 \det\left(\mathbf{A}_{R,m} - \mathbf{B}_{R,m}^H \mathbf{J}_R\right)$$
$$- \log_2\left(1 + |\lambda_{E,m}|^2 (1 - \overline{v}_{E,m1}v_{E,m1})\right)$$
$$- 2|\lambda_{E,m}|\right) - \log_2 \det\left(\mathbf{A}_{E,m}\right).$$

Proof: The proof is provided in Appendix C. ∎

Case $Tr(\mathbf{J}_R) \neq 0$ and $Tr(\mathbf{J}_E) \neq 0$: Namely, both $\mathbf{J}_R$ and $\mathbf{J}_E$ are diagonalizable. Before presenting the optimal solution conclusion for this case, we firstly introduce a lemma as below.

Lemma 5: For function $f(x) = (a + b\cos x)/[c + d\cos(x + \omega)]$ with $a > b > 0$, $c > d > 0$, $\omega \in [0, 2\pi)$, and the variable $x \in [0, 2\pi)$, we have,

(i) If $\omega \in [0, \pi)$, for $\forall x \in [0, 2\pi)$, $\exists \hat{x} \in [0, \pi - \omega]$ satisfies $f(\hat{x}) \geq f(x)$, i.e., for $\forall x \in [0, 2\pi)$, there always exists a optimal solution $\hat{x} \in [0, \pi - \omega]$ maximizes $f(x)$;

(ii) If $\omega \in [\pi, 2\pi)$, for $\forall x \in [0, 2\pi)$, $\exists \hat{x} \in [3\pi - \omega, 2\pi]$ satisfies $f(\hat{x}) \geq f(x)$, i.e., for $\forall x \in [0, 2\pi)$, there always exists a optimal solution[2] $\hat{x} \in [3\pi - \omega, 2\pi]$ maximizes $f(x)$.

Proof: The proof is provided in Appendix D. ∎

Based on the Lemma 5, let $\alpha_R = 1 + |\lambda_{R,m}|^2(1 - \overline{v}_{R,m1}v_{R,m1})$, $\beta_R = 2|\lambda_{R,m}|$, $\alpha_E = 1 + |\lambda_{E,m}|^2(1 - \overline{v}_{E,m1}v_{E,m1})$, $\beta_E = 2|\lambda_{E,m}|$, $\varphi_m = \arg(\theta_m)$, $\varphi_{\lambda_{R,m}} = \arg(\lambda_{R,m})$, $\varphi_{\lambda_{E,m}} = \arg(\lambda_{E,m})$, then $\overline{R}_{sec}(\theta_m)$ is rewritten as

$$\overline{R}_{sec}(\theta_m) = \log_2\left(1 + |\lambda_{R,m}|^2 (1 - \overline{v}_{R,m1}v_{R,m1})\right.$$
$$+ 2\Re\{\theta_m \lambda_{R,m}\}\right) - \log_2\left(1 + |\lambda_{E,m}|^2\right.$$
$$\times \left(1 - \overline{v}_{E,m1}v_{E,m1}\right) + 2\Re\{\theta_m \lambda_{E,m}\}\right)$$
$$= \log_2\left(\frac{\alpha_R + \beta_R \cos(\varphi_m + \varphi_{\lambda_{R,m}})}{\alpha_E + \beta_E \cos(\varphi_m + \varphi_{\lambda_{E,m}})}\right)$$
$$\triangleq \log_2(f(\varphi_m)). \tag{26}$$

Now, for problem (18), maximizing $\overline{R}_{sec}(\theta_m)$ is equivalent to maximize $f(\varphi_m)$. Moreover, in (26), we have $1 + |\lambda_{R,m}|^2(1 - \overline{v}_{R,m1}v_{R,m1}) + 2\Re\{\theta_m \lambda_{R,m}\} > 0$ and $1 + |\lambda_{E,m}|^2(1 - \overline{v}_{E,m1}v_{E,m1}) + 2\Re\{\theta_m \lambda_{E,m}\} > 0$ for $\forall \theta_m$, namely, $\alpha_R > \beta_R > 0$ and $\alpha_E > \beta_E > 0$. Hence, the corresponding optimal solution can be characterized by the Proposition 6 as below and the proof is omitted for it can be easily proved from the Lemma 5.

---

[2]Herein, the variable x can take the value of 2π in the optimal interval, however, the definition domain of the $f(x)$ is a right-open interval, i.e., $x \in [0, 2\pi)$. In fact, it is not conflict with each other as $f(2\pi) = f(0)$.

Proposition 6: If $Tr(\mathbf{J}_R) \neq 0$ and $Tr(\mathbf{J}_E) \neq 0$, the optimal solution for (18) is over the interval defined as below,

(i) If $\text{mod}(\varphi_{\lambda_{E,m}} - \varphi_{\lambda_{R,m}}, 2\pi) \in [0, \pi)$, the optimal phase $\hat{\varphi}_m \in [-\varphi_{\lambda_{R,m}}, \pi - \varphi_{\lambda_{E,m}}]$;

(ii) If $\text{mod}(\varphi_{\lambda_{E,m}} - \varphi_{\lambda_{R,m}}, 2\pi) \in [\pi, 2\pi)$, the optimal phase $\hat{\varphi}_m \in [3\pi - \varphi_{\lambda_{E,m}}, 2\pi - \varphi_{\lambda_{R,m}}]$. In which, $\text{mod}(x, y)$ represents the remainder of variable x over y. ∎

Based on the Proposition 6, we can then perform the linear search to obtain the optimal solution for problem (18) under the condition $Tr(\mathbf{J}_R) \neq 0$ and $Tr(\mathbf{J}_E) \neq 0$.

To summarize the above analysis, for problem (18), its optimal solution can be characterized as below

$$\hat{\theta}_m = \begin{cases} 1, & Tr(\mathbf{J}_R) = 0, \ Tr(\mathbf{J}_E) = 0 \\ e^{-j\arg(\lambda_{R,m})}, & Tr(\mathbf{J}_R) \neq 0, \ Tr(\mathbf{J}_E) = 0 \\ e^{j(\pi - \arg(\lambda_{E,m}))}, & Tr(\mathbf{J}_R) = 0, \ Tr(\mathbf{J}_E) \neq 0 \\ \overline{\theta}_m, & Tr(\mathbf{J}_R) \neq 0, \ Tr(\mathbf{J}_E) \neq 0 \end{cases} \tag{27}$$

where $\overline{\theta}_m$ is obtained by linear search. Therefore, we formulate the algorithm for OP3 as below, i.e., the Algorithm 2.

Algorithm 2 Optimize IRS Reflection Coefficients

S1: Initialize: Randomly generate $\{\theta_m^0\}_{m=1}^M$, $\varepsilon > 0$, $n = 0$;

S2: Obtain $\hat{\theta}_m^n$, $m = 1, 2, \ldots, M$ by turns according to (27);

S3: If $\sum_{m=1}^M |\hat{\theta}_m^n - \theta_m^n| > \varepsilon$, set $\{\theta_m^{n+1} = \hat{\theta}_m^n\}_{m=1}^M$, $n = n + 1$, go back to S2; else set $\{\hat{\theta}_m = \theta_m^n\}_{m=1}^M$;

S4: Output $\{\hat{\theta}_m\}_{m=1}^M$;

In Algorithm 2, $\{\hat{\theta}_m^n\}_{m=1}^M$ denotes the solution obtained in the nth iteration. The core idea of the algorithm is that, we alternatively optimize θ_m for given θ_i, $i = 1, \ldots, M$, $i \neq m$. In addition, the optimization of θ_m is following the rule of (27). Furthermore, since the original problem is bounded and the progress of the alternative optimization is monotonically non-decreasing, thus the above algorithm is surely convergent.

C. OVERALL ALGORITHM

In this subsection, the overall algorithm for OP1 is provided. As mentioned, the algorithm is based on alternating optimization, which optimize the objective function with respect to different subsets of optimization variables in each iteration while the other subsets are fixed. Therefore, it is summarized as the Algorithm 3 as follows. where $\hat{\mathbf{Q}}_s^n$ and $\{\hat{\theta}_m^n\}_{m=1}^M$ denote the stationary points obtained by the Algorithm 1 and Algorithm 2 in the nth iteration of the Algorithm 3, respectively. The procedures of the algorithm are as follows: firstly, we randomly generate a set of $\{\theta_m^0\}_{m=1}^M$ with $|\theta_m^0| = 1$, $\forall m$ and the phases of θ_m^0 are following the uniform

Algorithm 3 Alternating Optimization Based Algorithm

S1: Initialize: Randomly generate $\{\theta_m^0\}_{m=1}^M$, $\tilde{\mathbf{Q}}_s^0 \succcurlyeq 0$, $\varepsilon > 0$, $n = 0$;

S2: Obtain $\hat{\mathbf{Q}}_s^n$ with given $\{\theta_m^n\}_{m=1}^M$ and $\tilde{\mathbf{Q}}_s^n$ by Algorithm 1;

S3: Obtain $\left\{\hat{\theta}_m^n\right\}_{m=1}^M$ with $\hat{\mathbf{Q}}_s^n$ by Algorithm 2;

S4: If $\displaystyle\sum_{m=1}^M \left|\hat{\theta}_m^n - \theta_m^n\right| > \varepsilon$, set $\left\{\theta_m^{n+1} = \hat{\theta}_m^n\right\}_{m=1}^M$, $\tilde{\mathbf{Q}}_s^{n+1} = \hat{\mathbf{Q}}_s^n$,

$n = n + 1$, go back to S2; else set $\left\{\hat{\theta}_m = \theta_m^n\right\}_{m=1}^M$ and $\hat{\mathbf{Q}}_s = \hat{\mathbf{Q}}_s^n$;

S5: Output $\left\{\hat{\theta}_m\right\}_{m=1}^M$ and $\hat{\mathbf{Q}}_s$.

distribution over $[0, 2\pi)$. Secondly, for given the reflecting coefficients at the IRS and based on the Algorithm 1, we optimize the transmit covariance matrix at the AP. Thirdly, with the optimized transmit covariance matrix at the AP and based on the Algorithm 2, we optimize the reflecting coefficients at the IRS. Finally, the above two steps are iteratively performed until it is converged. Apparently, duo to the monotonic non-decreasing properties of the Algorithm 1 and the Algorithm 2, and also the objective function in OP1 is bounded, then the overall algorithm is surly converged.

Furthermore, we analyze the computational complexity of the proposed algorithm in the worst case. The complexity of the Algorithm 1 mainly depends on the convex approximation and the process of solving the convex problem (12), for which has the complexity of $O\left(I_1\left(N_E^3 + N_T^6\right)\right)$ [39]. In which, I_1 denotes the iteration number of Algorithm 1. The computational complexity of the Algorithm 2 comes from the computing of matrix inversion and one-dimensional search, which can be indicated as $O\left(I_2 M\left(N_R^3 + N_E^3 - log_2\varepsilon\right)\right)$. Herein, $\varepsilon \in (0, 1)$ and I_2 represent the accuracy of binary search and the iteration number of Algorithm 2, respectively. Therefore, the complexity of the overall algorithm is $O\left(I_3\left(I_1\left(N_E^3 + N_T^6\right) + I_2 M\left(N_R^3 + N_E^3 - log_2\varepsilon\right)\right)\right)$, and I_3 represents the iteration number of Algorithm 3.

D. EXTENDED TO DISCRETE MODEL

In the previous discussion, we assume that the phase of IRS reflecting element is continuously adjustable, which is too ideal to achieve in practical. And existing studies showed that [3], [21], the IRS only can adjust the phase with limited accuracy due to the hardware limitations. To ensure the practicability of the proposed algorithm in more practical application scenarios, the IRS discrete reflecting coefficient model is discussed briefly. In particular, replacing the Φ_1 with Φ_2 in OP1, which formulates the problem OP4 as below.

$$\max_\Theta R_{sec}(\Theta)$$

$$= \log_2 \det\left(\mathbf{I}_{N_R} + \frac{1}{\sigma_R^2}\mathbf{G}_{TR}(\Theta)\mathbf{Q}_s\mathbf{G}_{TR}^H(\Theta)\right)$$

$$- \log_2 \det\left(\mathbf{I}_{N_E} + \frac{1}{\sigma_E^2}\mathbf{G}_{TE}(\Theta)\mathbf{Q}_s\mathbf{G}_{TE}^H(\Theta)\right)$$

$$s.t.\, \theta_m \in \Phi_2, \quad m = 1, 2, \ldots, M \tag{28}$$

Note that, OP4 belongs to the mixed integer nonlinear programming (MINLP), which is an NP-hard problem and difficult to handle. Hence, the heuristic projection method is used here to solve this problem [21]. That is, we denote the solution of IRS reflecting coefficients for OP1 and OP4 are $\mathbf{v}_s = [\theta_{s,1}, \theta_{s,2}, \ldots, \theta_{s,M}]$ and $\mathbf{v}_d = [\theta_{d,1}, \theta_{d,2}, \ldots, \theta_{d,M}]$, respectively. Then $\mathbf{v}_d$ is provided by

$$\theta_{d,m} = \theta_{\hat{q}}, \hat{q} = \arg\min_{0 \leq q < Q} \left|\theta_{s,m} - e^{j\varphi_q}\right|, \quad m = 1, 2, \ldots, M \tag{29}$$

Therefore, we obtain the suboptimal algorithm for the discrete model, i.e., solving the OP4. In fact, the algorithm for OP4 is the same as that for OP1, i.e., the Algorithm 3, except that right now, after the Algorithm 3 is convergent, we have to perform the projection operation via following (29) to obtain the achievable discrete IRS reflecting coefficients.

Remark: Note that, the reflection amplitude and phase shifts are uncorrelated in the considered IRS reflecting coefficient model Φ_1 and Φ_2. In practice, however, they may be coupled and not be simply expressed as Φ_1 and Φ_2, as shown in the most recent works e.g., [19]. And the AO-based algorithm proposed in the paper can be extended to this case with some modification. Specifically, given the IRS reflection coefficients, the SCA-based method proposed in the Algorithm 1 is used to optimize the transmit covariance matrix. Then, given the transmit covariance matrix, the AO is adopted again to optimize IRS reflection coefficients by turn. Finally, the above two steps are iteratively performed until it is converged. For the optimization of a single IRS reflection coefficient, the approximate solution can be obtained numerically via a one-dimensional search over $[-\pi, \pi]$ but not a closed-form solution or an optimal interval, which is different from the Algorithm 3.

IV. SIMULATION ANALYSIS

In this section, the performance of the proposed algorithms are evaluated by numerical simulation. Considering two scenarios, they are, the strength of legitimate channel is superior or inferior to the eavesdropping channel. In the former case, the AP, legitimate user, eavesdropper and the IRS are located at (0, 0), (45, 0), (55, 0) and (50, 5) in meter (m) in a two-dimensional plane, respectively. And the latter exchanges the coordinates of the legitimate user with the eavesdropper. The other system parameters used in the simulations are following [40] and [41], that is, we set the antenna number of all nodes as 4, namely, $N_T = N_R = N_E = 4$. The noise power at both the legitimate receiver and the eavesdropper is set as $\sigma_R^2 = \sigma_E^2 = -40dBm$ and the maximum total transmitted power is set as $P_{\max} = 30dBm$.

Without loss of generality, all the channels are modeled as [8]

$$\mathbf{H} = \sqrt{\beta/\kappa + 1} \left(\sqrt{\kappa} \mathbf{H}^{LoS} + \mathbf{H}^{NLoS} \right),$$

where κ is the Rician factor, while $\mathbf{H}^{LOS}$ and $\mathbf{H}^{NLOS}$ represent the deterministic line-of-sight (LoS) and Rayleigh fading/non-LoS (NLoS) components, respectively. β represents the path loss, and is given by $\beta = \beta_0 - 10\alpha \log_{10}(d/d_0)$. Herein, β_0 denotes the path loss at the reference distance $d_0 = 1m$, α and d represent the path loss exponent and the distance between the corresponding nodes, e.g., between AP and the IRS, or between AP and the legitimate user. Similar to [25], we assume that the channels from IRS to legitimate user and the eavesdropper have LoS component and experience Rayleigh fading, simultaneously, however, the channels from AP to legitimate user, eavesdropper and IRS, only experience Rayleigh fading. Hence, the Rician factors are set as $\kappa_{SR} = \kappa_{SE} = 1$ and $\kappa_{TR} = \kappa_{TE} = \kappa_{TS} = 0$. In addition, path loss exponents of all channels are set as $\alpha_{TR} = \alpha_{TE} = \alpha_{TS} = \alpha_{SR} = \alpha_{SE} = 2$.

Furthermore, in order to better understand the positive effects of the IRS in improving the secure communication performance for the MIMOME system and the performance gain of the proposed algorithms, some benchmark schemes are introduced in the simulation based performance comparison and analysis. Thus, following four algorithms are evaluated in the simulations, i.e., no-IRS, random-IRS, AO-based-IRS with $b = 1$(or 3, 5) bits and the AO-based-IRS continues with $p = 1$ (or 10, 20, 40).

no-IRS: That is, no IRS is used in the system and the secrecy rate is obtained by directly optimizing (9) under the conditions $\mathbf{G}_{TR}(\Theta) = \mathbf{H}_{TR}$ and $\mathbf{G}_{TE}(\Theta) = \mathbf{H}_{TE}$.

random-IRS: That is, the reflecting coefficients of the IRS are randomly generated via following the rules that $|\theta_m| = 1, m = 1,.., M$ and θ_m follows an independent uniform distribution over $[0, 2\pi)$.

AO-based-IRS continues with $p = 1$ (or 10, 20, 40): It is our proposed alternative optimization based algorithm, i.e., the Algorithm 3 with one or multiple initial points. And p (=1 or 10, 20, 40) denotes the number of initial points used for this algorithm.

AO-based-IRS with $b = 1$ (or 3, 5) bits: It is based on the Algorithm 3 with one initial point, except that right now, the reflecting coefficients can only take finitely discrete value and b denotes the number of quantization bits, which determines the number of quantized reflection coefficient values of the IRS elements, i.e., $Q = 2^b$.

At first, under the condition that the legitimate user channel (from AP to the legitimate user) is superior to the eavesdropper channel (from AP to the eavesdropper), the achievable secrecy rate of different algorithms are evaluated by varying the available transmission power constraint at the AP, i.e., the $P_{max} \in [0.2, 2]W$ and $M = 20$, and the result is shown in Fig. 2. One can note that, with the increase of the available transmission power at the AP, the achievable secrecy rates for all these algorithms are increased. This phenomenon is
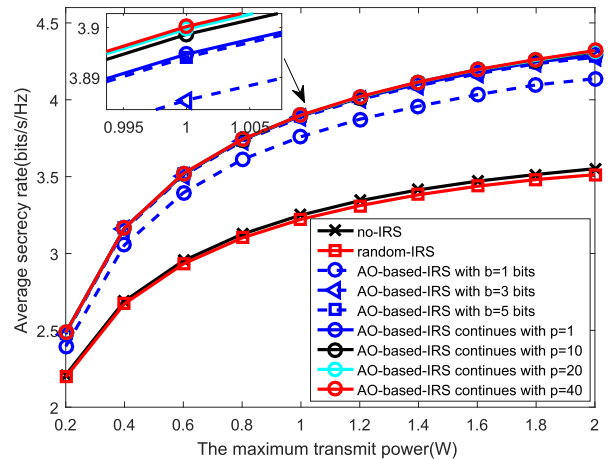

FIGURE 2. Average secrecy rate VS P_{max} (superior).

reasonable and it is consistent with the traditional MIMOME system [33]–[35]. In addition, from Fig. 2, it is surprising that, our proposed AO-based algorithm is not sensitive with the selection of the initial points, as the performance difference among the algorithm 'AO-based-IRS continues with $p = 1$ (or 10 20 40)' is negligible. However, it is noted that these AO-based algorithms, i.e., 'AO-based-IRS continues with $p = 1$ (or 10, 20, 40)' get larger secrecy rate over the other benchmark schemes, i.e., 'no-IRS', 'random-IRS' and 'AO-based-IRS with $b = 1$ (or 3, 5)bits'. Hence, in the following, for the algorithm performance evaluation, we only consider the case $p = 1$ for simplicity. Also for Fig. 2, we note that, for the AO-based algorithm with IRS but under different quantization bits about the reflecting coefficients, i.e., 'AO-based-IRS with $b = 1$ bits', 'AO-based-IRS with $b = 3$ bits' and 'AO-based-IRS with $b = 5$ bits' obtain less secrecy rate compared with the condition with continues-adjustable phases, and the algorithm 'no-IRS' and 'random-IRS' obtain the worst performance and they are pretty close. Moreover, on the one hand, with the increasing of the available transmission power at the AP, the performance gap between the algorithms 'AO-based-IRS with $b = x$ bits' and the algorithm 'AO-based-IRS continues with $p = 1$' becomes larger, on the other hand, through increasing the quantization bits of the reflecting coefficients at the IRS, the performance gap between the algorithms 'AO-based-IRS with $b = x$ bits' and the algorithm 'AO-based-IRS continues with $p = 1$' could be significantly reduced. It is indicated that taking $b = 3$ bits is sufficient for the system to obtain an acceptable secrecy rate with ignorable performance loss, i.e., less than $0.02 bits/s/Hz$ even at $P_{max} = 2W$, via comparing with the algorithm 'AO-based-IRS continues with $p = 1$'. Therefore, in the following, for the algorithms 'AO-based-IRS with $b = x$ bits', we only consider the case $b = 3$ bits.

Then, with the same simulation parameters but under the condition that the legitimate channel is inferior to the eavesdropper channel, the achievable secrecy rate of different
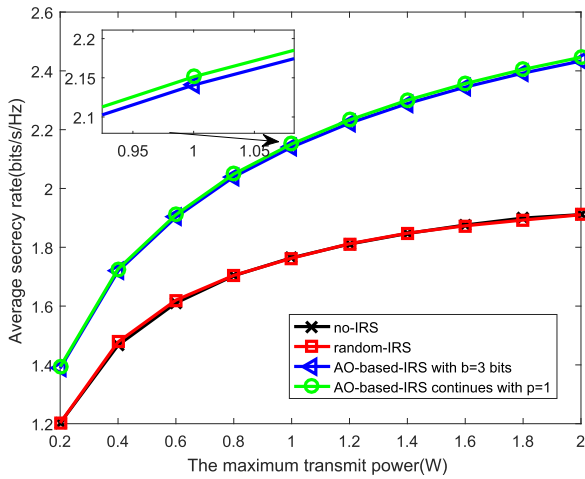
FIGURE 3. Average secrecy rate VS P_{max} (inferior).

algorithms are evaluated again through changing the available transmission power constraint at the AP and the result is shown in Fig. 3. We can observe that, as expected, all the algorithms' obtained average secrecy rate is significantly reduced, however, the tendencies of the secrecy rate performance obtained by these algorithms are the same as that the legitimate channel is superior to the eavesdropper channel shown in Fig. 2, i.e., the algorithm 'AO-based-IRS continues with $p = 1$' obtains the largest secrecy rate, then it is the algorithm 'AO-based-IRS with $b = 3$ bits', and still the algorithm 'no-IRS' and 'random-IRS' have the similar performance with the least secrecy rate.
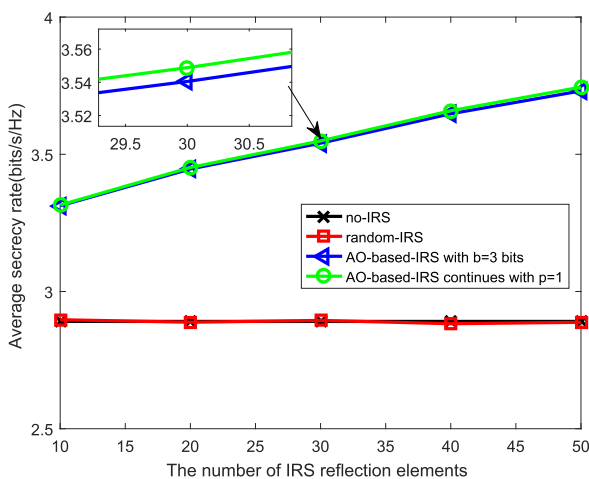

FIGURE 4. Average secrecy rate VS number of IRS elements.

In Fig. 4, we further analyze how the system achievable secrecy rate performance is affected by the number of IRS elements in the system, i.e., from $M = 10$ to 50. Herein, still based on the condition that the legitimate channel is superior to the eavesdropper channel and the other simulation parameters are the same as that used in the Fig. 2. One can note that, for both the algorithm 'AO-based-IRS with $b = 3$ bits' and

the algorithm 'AO-based-IRS continues with $p = 1$', their achievable secrecy rates are linear increment with the number of the IRS elements in the system. This increment comes from the factor more IRS elements in the system, more signal paths and energy could be reflected by the IRS to enhance the signal quality at the legitimate user but to reduce the signal quality at the eavesdropper. In addition, as expected, the performance of the algorithm 'no-IRS' and 'random-IRS' are not affected by the number of the IRS elements in the system.
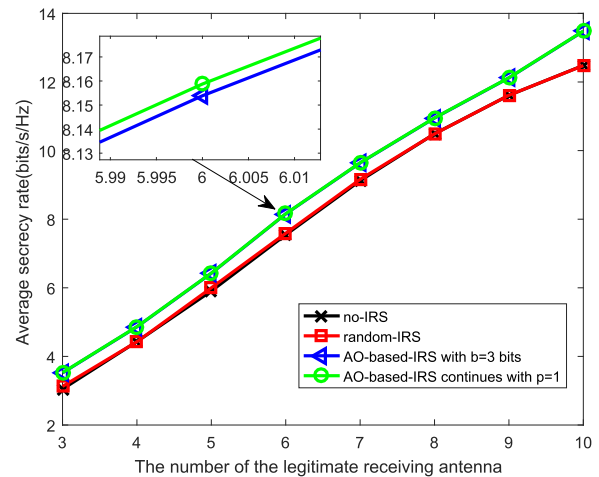

FIGURE 5. Average secrecy rate VS number of legitimate receiving antennas.

Next, in Fig. 5, the system achievable secrecy rate performance of the proposed algorithms are evaluated through changing the number of the legitimate receiving antennas, i.e., from $N_R = 3$ to 10, with given $N_T = 10$ and $N_E = 6$. As expected, with the increase of the number of the legitimate receiving antennas, the secrecy rate of all the algorithm are increased. This phenomenon comes from the following fact: the increase of the number of the legitimate receiving antennas can bring greater spatial diversity gain to the legitimate user, moreover, the rate of the legitimate user is increasing, as a result, the secrecy rate is increasing simultaneously. In addition, the performance of the algorithms 'AO-based-IRS continues with $p = 1$' and 'AO-based-IRS with $b = 3$ bits' is quite close, as well as the performance of the algorithms 'no-IRS' and 'random-IRS', which further verifies the above conclusion.

To measure the performance loss of the proposed heuristic solution with the stationary solution, a benchmark schem is introduced, namely, 'AO-based-IRS with exhaustive search' which takes exhaustive search to obtain the optimal IRS reflection coefficients for given transmit covariance matrix. In Fig. 6, the system achievable secrecy rate performance of algorithms 'AO-based-IRS continues with p=1' and 'AO-based-IRS with exhaustive search' are evaluated by varying the available transmission power constraint at the AP, i.e., the $P_{max} \in [0.2, 2]W$ and $M = 10$. One can note that, as expected, with the increase of the available
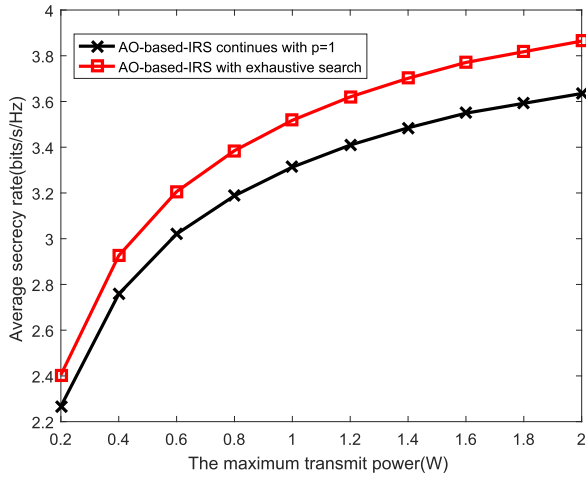
FIGURE 6. Average secrecy rate VS P_{max} (superior).

transmission power at the AP, the achievable secrecy rates for both algorithms are increased. In addition, from Fig. 6, we note that 'AO-based-IRS with exhaustive search' gets better average secrecy rate performance over the 'AO-based-IRS continues with p=1', and the performance gap between these two algorithms becomes larger with the increasing of the available transmission power at the AP. However, it is gratifying that the proposed algorithm is good enough to assume less than $0.2 bits/s/Hz$ performance loss even at $P_{max} = 2W$.
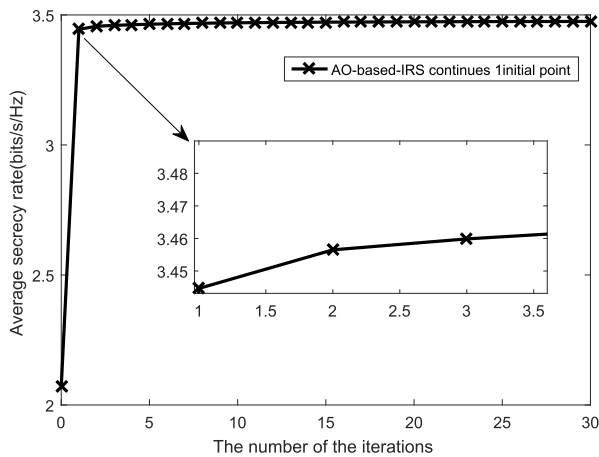

FIGURE 7. Average secrecy rate VS number of the iterations.

Finally, the convergence behavior of the proposed algorithm is evaluated and the result is shown in Fig. 7. Herein, the simulation parameters used in Fig. 7 are the same as that adopted in Fig. 2. However, for simplicity, we only consider the situation of $p = 1$, i.e., we testify the algorithm 'AO-based-IRS continues with $p = 1$'. From which, we note that, the proposed algorithm can converge quickly, i.e., no more than 10 outer iterations can surely promise the convergence of the AO algorithm, and this phenomenon validates our analysis in Section III.

V. CONCLUSION

In this paper, the joint optimization of the transmit covariance matrix at the AP and the reflecting coefficients at the IRS to maximize the secrecy rate for the IRS-MIMOME system has been proposed and solved, with two different assumptions on the phase shifting capabilities at the IRS, i.e., the IRS has the continuous reflecting coefficients and the IRS has the discrete reflecting coefficients. For the former, due to the non-convexity of the formulated problem, an AO based algorithm has been proposed, i.e., for given the reflecting coefficients at the IRS, the SCA-based algorithm has been used to solve the transmit covariance matrix optimization, while given the transmit covariance matrix at the AP, alternative optimization has been used again in individually optimizing of each reflecting coefficient (i.e., θ_m) at the IRS with the fixed of the other reflecting coefficients (i.e., $\theta_i, i = 1, \ldots, M, i \neq m$). For the individual reflecting coefficient optimization, the closed-form or an interval of the optimal solution has been provided. Then, the overall algorithm has been extended to the discrete reflecting coefficient model at the IRS. Finally, from the numerical simulation evaluation, we have demonstrated that the proposed AO-based algorithm outperforms the other benchmark schemes. It has been also indicated that, for the IRS-MIMOME system, for practical IRS system with the discrete reflecting coefficient, taking $Q = 8$ is sufficient for the system to experience less than $0.02 bits/s/Hz$ performance loss even at $P_{max} = 2W$ and with more than 20 IRS elements.

It is important to note that, in this paper, only one legitimate user and one eavesdropper are considered in the system, therefore, the more practical scenario with multiple legitimate users and multiple eavesdroppers would be concerned. In addition, in the system, the AP may use the AN to further improve the secrecy rate performance for the legitimate users. It is interesting and worth further studying the transmission strategies for these systems. Furthermore, due to large reflection elements for the IRS and multiple antennas at the transceivers, therefore, the perfect CSI assumption is impractical and it is more practical to investigate the case with imperfect CSI in the future.

APPENDIX A
THE LAGRANGE DUAL PROBLEM OF (12)
Here, we provide the Lagrange dual problem of (12). That is, the KarushíCKuhníCTucker (KKT) conditions [39] for the above convex approximation problem are, namely,

$$\begin{cases} \dfrac{1}{ln2}\dfrac{1}{\sigma_R^2}\mathbf{G}_{TR}^H\mathbf{W}_R^{-1}\mathbf{G}_{TR} - \dfrac{1}{ln2}\dfrac{1}{\sigma_E^2}\mathbf{G}_{TE}^H\mathbf{W}_{E,\tilde{\mathbf{Q}}_s}^{-1}\mathbf{G}_{TE} \\ -\lambda\mathbf{I}_{N_T} + \mathbf{Z}^T = 0 \\ \lambda\left[Tr\left(\mathbf{Q}_s\right) - P_{max}\right] = 0\,. \end{cases} \quad (30)$$

Herein, $\mathbf{W}_R = \mathbf{I}_{N_R} + \frac{1}{\sigma_R^2}\mathbf{G}_{TR}\mathbf{Q}_s\mathbf{G}_{TR}^H$. $\lambda \geq 0$ and $\mathbf{Z} \succeq 0$ are the dual variables associated with the transmission power constraint and the positive semi-definite constraint on the $\mathbf{Q}_s$, respectively. Correspondingly, the Lagrangian

function of (12) can be written as

$$L\left(\mathbf{Q}_s, \lambda, \mathbf{Z}\right) = -\tilde{R}_{sec} + \lambda\left[Tr\left(\mathbf{Q}_s\right) - P_{\max}\right] - Tr\left[\mathbf{Z}\mathbf{Q}_s\right] \quad (31)$$

Since problem (12) is convex and satisfies the Slater's condition, the duality gap is zero between (12) and its dual problem. Thus, the optimal solution of (12) can be determined via solving the following Lagrange dual problem

$$\min_{\lambda \geq 0} \; g\left(\lambda\right). \quad (32)$$

Herein,

$$g\left(\lambda\right) = \max_{\mathbf{Q}_s \succcurlyeq 0} \left\{ \tilde{R}_{sec} - \lambda\left[Tr\left(\mathbf{Q}_s\right) - P_{\max}\right] \right\}. \quad (33)$$

APPENDIX B
PROOF OF PROPOSITION 3

Proof: Since $Tr\left(\mathbf{J}_R\right) \neq 0$ and $Tr\left(\mathbf{J}_E\right) = 0$, then the objective function in (18) is transformed to (24) and the problem is equivalent to maximize $\Re\left\{\theta_m \lambda_{E,m}\right\}$ in (24). In addition, $\Re\left\{\theta_m \lambda_{R,m}\right\} \leq \left|\theta_m \lambda_{R,m}\right| = \left|\theta_m\right|\left|\lambda_{R,m}\right| = \left|\lambda_{R,m}\right|$, and the inequality holds with equality if and only if $\hat{\theta}_m = e^{-j\arg(\lambda_{R,m})}$, thus we have the optimal solution conclusion for (18). Furthermore, the corresponding optimal value can be obtained by substituting $\hat{\theta}_m = e^{-j\arg(\lambda_{R,m})}$ into (17). That is, we have the proposition. ∎

APPENDIX C
PROOF OF PROPOSITION 4

Proof: Since $Tr\left(\mathbf{J}_R\right) = 0$ and $Tr\left(\mathbf{J}_E\right) \neq 0$, then the objective function in (18) is transformed to (25) and the problem is equivalent to minimize $\Re\left\{\theta_m \lambda_{E,m}\right\}$ in (25). Since $\Re\left\{\theta_m \lambda_{E,m}\right\} \geq -\left|\theta_m \lambda_{E,m}\right| = -\left|\theta_m\right|\left|\lambda_{E,m}\right| = -\left|\lambda_{E,m}\right|$, where the inequality holds with equality if and only if $\hat{\theta}_m = e^{j(\pi - \arg(\lambda_{E,m}))}$, thus we have the optimal solution conclusion for (18). Furthermore, the corresponding optimal value can be obtained by substituting $\hat{\theta}_m = e^{j(\pi - \arg(\lambda_{E,m}))}$ into (17). Therefore, we have this proposition. ∎

APPENDIX D
PROOF OF LEMMA 5

Proof: Herein, for the Lemma 5, we only present the proof of the conclusion (i) and the conclusion (ii) could be proved in the same manner thus it is omitted here for simplification. At first, we have

$$f(x) = \frac{a + b\cos x}{c + d\cos(x + \omega)}, \quad x \in [0, 2\pi) \quad (34)$$

Since $a > b > 0$, $c > d > 0$ and $\omega \in [0, \pi)$, we know that $f_1(x) = a + b\cos x$ takes extremum at $x = 0, \pi, 2\pi$ and $f_2(x) = c + d\cos(x + \omega)$ takes extremum at $x = \pi - \omega$, $2\pi - \omega$ over $x \in [0, 2\pi)$. Following that, we can divided the definition domain of the function $f(x)$ into four regions, i.e., $D_1 = [0, \pi - \omega]$, $D_2 = (\pi - \omega, \pi)$, $D_3 = [\pi, 2\pi - \omega)$ and $D_4 = [2\pi - \omega, 2\pi)$. Then we prove that, for function $f(x), x \in [0, 2\pi)$, it can take the maximization only at $x \in [0, \pi - \omega]$ if $\omega \in [0, \pi)$, that is, for $\forall x \in D_i, i = 2, 3, 4$, $\exists \hat{x} \in D_1$ satisfies $f(\hat{x}) > f(x)$. The proof is as follows.

Case $\forall x \in D_2$: Let $\hat{x}_1 = \pi - \omega \in D_1$, then for $\omega \in [0, \pi)$ we always have $\cos x < \cos \hat{x}_1$ and $\cos(x + \omega) > \cos(\hat{x}_1 + \omega)$, due to $a > b > 0$ and $c > d > 0$, then from the definition of $f(x)$ we know that $f(x) < f(\hat{x}_1)$.

Case $\forall x \in D_3 \bigcup D_4$: Let $\hat{x}_2 = 2$ $textpi - x \in [0, \pi]$, then for $\omega \in [0, \pi)$ we always have $\cos x = \cos \hat{x}_2$ and $\cos(x + \omega) > \cos(\hat{x}_2 + \omega)$ due to $\cos x = \cos \hat{x}_2$ and $\sin x < \sin \hat{x}_2$; also since $a > b > 0$ and $c > d > 0$, then we have $f(x) < f(\hat{x}_2)$ from the definition of $f(x)$.

To sum up the case $\forall x \in D_2$ and case $\forall x \in D_3 \bigcup D_4$, we have the conclusion that the optimal solution $\hat{x} \in D_1$. Therefore, the conclusion (i) of the Lemma 5 is proved and in the same manner, we can also prove the conclusion (ii) of the Lemma 5. Finally, we have the Lemma 5. ∎

## REFERENCES

[1] X. Chen, D. W. K. Ng, W. H. Gerstacker, and H.-H. Chen, "A survey on multiple-antenna techniques for physical layer security," *IEEE Commun. Surveys Tuts.*, vol. 19, no. 2, pp. 1027–1053, 2nd Quart., 2017.

[2] D. Wang, B. Bai, W. Zhao, and Z. Han, "A survey of optimization approaches for wireless physical layer security," *IEEE Commun. Surveys Tuts.*, vol. 21, no. 2, pp. 1878–1911, 2nd Quart., 2019.

[3] C. Liaskos, S. Nie, A. Tsioliaridou, A. Pitsillides, S. Ioannidis, and I. Akyildiz, "A new wireless communication paradigm through software-controlled metasurfaces," *IEEE Commun. Mag.*, vol. 56, no. 9, pp. 162–169, Sep. 2018.

[4] H. Yang, X. Cao, F. Yang, J. Gao, S. Xu, M. Li, X. Chen, Y. Zhao, Y. Zheng, and S. Li, "A programmable metasurface with dynamic polarization, scattering and focusing control," *Sci. Rep.*, vol. 6, no. 1, p. 35692, Dec. 2016.

[5] M. D. Renzo, M. Debbah, D.-T. Phan-Huy, A. Zappone, M.-S. Alouini, C. Yuen, V. Sciancalepore, G. C. Alexandropoulos, J. Hoydis, H. Gacanin, J. D. Rosny, A. Bounceur, G. Lerosey, and M. Fink, "Smart radio environments empowered by reconfigurable AI meta-surfaces: An idea whose time has come," *EURASIP J. Wireless Commun. Netw.*, vol. 2019, no. 1, p. 129, Dec. 2019.

[6] Q. Wu and R. Zhang, "Towards smart and reconfigurable environment: Intelligent reflecting surface aided wireless network," *IEEE Commun. Mag.*, vol. 58, no. 1, pp. 106–112, Jan. 2020.

[7] Q. Wu and R. Zhang, "Intelligent reflecting surface enhanced wireless network: Joint active and passive beamforming design," in *Proc. IEEE Global Commun. Conf. (GLOBECOM)*, Abu Dhabi, United Arab Emirates, Dec. 2018, pp. 1–6.

[8] Q. Wu and R. Zhang, "Intelligent reflecting surface enhanced wireless network via joint active and passive beamforming," *IEEE Trans. Wireless Commun.*, vol. 18, no. 11, pp. 5394–5409, Nov. 2019.

[9] C. Huang, A. Zappone, M. Debbah, and C. Yuen, "Achievable rate maximization by passive intelligent mirrors," in *Proc. IEEE Int. Conf. Acoust., Speech Signal Process. (ICASSP)*, Calgary, AB, Canada, Apr. 2018, pp. 3714–3718.

[10] Q. Wu and R. Zhang, "Beamforming optimization for wireless network aided by intelligent reflecting surface with discrete phase shifts," *IEEE Trans. Commun.*, vol. 68, no. 3, pp. 1838–1851, 2020.

[11] C. Huang, A. Zappone, G. C. Alexandropoulos, M. Debbah, and C. Yuen, "Large intelligent surfaces for energy efficiency in wireless communication," 2018, *arXiv:1810.06934*. [Online]. Available: http://arxiv.org/abs/1810.06934

[12] C. Huang, G. C. Alexandropoulos, A. Zappone, M. Debbah, and C. Yuen, "Energy efficient multi-user MISO communication using low resolution large intelligent surfaces," in *Proc. IEEE Globecom Workshops (GC Wkshps)*, Abu Dhabi, United Arab Emirates, Dec. 2018, pp. 1–6.

[13] Y. Han, W. Tang, S. Jin, C.-K. Wen, and X. Ma, "Large intelligent surface-assisted wireless communication exploiting statistical CSI," *IEEE Trans. Veh. Technol.*, vol. 68, no. 8, pp. 8238–8242, Aug. 2019.

[14] A. Taha, M. Alrabeiah, and A. Alkhateeb, "Enabling large intelligent surfaces with compressive sensing and deep learning," 2019, *arXiv:1904.10136*. [Online]. Available: http://arxiv.org/abs/1904.10136

[15] C. Huang, G. C. Alexandropoulos, C. Yuen, and M. Debbah, "Indoor signal focusing with deep learning designed reconfigurable intelligent surfaces," in *Proc. IEEE 20th Int. Workshop Signal Process. Adv. Wireless Commun. (SPAWC)*, Cannes, France, Jul. 2019, pp. 1–5.

[16] X. Tan, Z. Sun, J. M. Jornet, and D. Pados, "Increasing indoor spectrum sharing capacity using smart reflect-array," in *Proc. IEEE Int. Conf. Commun. (ICC)*, Kuala Lumpur, Malaysia, May 2016, pp. 1–6.

[17] X. Tan, Z. Sun, D. Koutsonikolas, and J. M. Jornet, "Enabling indoor mobile millimeter-wave networks based on smart reflect-arrays," in *Proc. IEEE INFOCOM Conf. Comput. Commun.*, Honolulu, HI, USA, Apr. 2018, pp. 270–278.

[18] G. Yang, X. Xu, and Y. Liang, "Intelligent reflecting surface assisted non-orthogonal multiple access," 2019, *arXiv:1907.03133*. [Online]. Available: http://arxiv.org/abs/1907.03133

[19] S. Abeywickrama, R. Zhang, and C. Yuen, "Intelligent reflecting surface: Practical phase shift model and beamforming optimization," 2019, *arXiv:1907.06002*. [Online]. Available: http://arxiv.org/abs/1907.06002

[20] X. Yu, D. Xu, and R. Schober, "Enabling secure wireless communications via intelligent reflecting surfaces," in *Proc. IEEE Global Commun. Conf. (GLOBECOM)*, Waikoloa, HI, USA, Dec. 2019, pp. 1–6.

[21] J. Chen, Y.-C. Liang, Y. Pei, and H. Guo, "Intelligent reflecting surface: A programmable wireless environment for physical layer security," *IEEE Access*, vol. 7, pp. 82599–82612, 2019.

[22] H. Shen, W. Xu, S. Gong, Z. He, and C. Zhao, "Secrecy rate maximization for intelligent reflecting surface assisted multi-antenna communications," *IEEE Commun. Lett.*, vol. 23, no. 9, pp. 1488–1492, Sep. 2019.

[23] B. Feng, Y. Wu, and M. Zheng, "Secure transmission strategy for intelligent reflecting surface enhanced wireless system," in *Proc. 11th Int. Conf. Wireless Commun. Signal Process. (WCSP)*, Xi'an, China, Oct. 2019, pp. 1–6.

[24] M. Cui, G. Zhang, and R. Zhang, "Secure wireless communication via intelligent reflecting surface," *IEEE Wireless Commun. Lett.*, vol. 8, no. 5, pp. 1410–1414, Oct. 2019.

[25] X. Guan, Q. Wu, and R. Zhang, "Intelligent reflecting surface assisted secrecy communication: Is artificial noise helpful or not?" 2019, *arXiv:1907.12839*. [Online]. Available: https://arxiv.org/abs/1907.12839

[26] D. Xu, X. Yu, Y. Sun, D. W. K. Ng, and R. Schober, "Resource allocation for secure IRS-assisted multiuser MISO systems," in *Proc. IEEE Globecom Workshops (GC Wkshps)*, Waikoloa, HI, USA, Dec. 2019, pp. 1–6.

[27] L. Subrt and P. Pechac, "Intelligent walls as autonomous parts of smart indoor environments," *IET Commun.*, vol. 6, no. 8, pp. 1004–1010, 2012.

[28] Q. Wu and R. Zhang, "Weighted sum power maximization for intelligent reflecting surface aided SWIPT," 2019, *arXiv:1907.05558*. [Online]. Available: http://arxiv.org/abs/1907.05558

[29] Z.-Q. He and X. Yuan, "Cascaded channel estimation for large intelligent metasurface assisted massive MIMO," *IEEE Wireless Commun. Lett.*, vol. 9, no. 2, pp. 210–214, Feb. 2020.

[30] H. Zhang, Y. Huang, S. Li, and L. Yang, "Energy-efficient precoder design for MIMO wiretap channels," *IEEE Commun. Lett.*, vol. 18, no. 9, pp. 1559–1562, Sep. 2014.

[31] E. Telatar, "Capacity of multi-antenna Gaussian channels," *Eur. Trans. Telecommun.*, vol. 10, no. 6, pp. 585–595, Nov. 1999.

[32] D. Park, "Secrecy sum rates of MIMO multi-receiver wiretap channels," *IEEE Commun. Lett.*, vol. 20, no. 9, pp. 1804–1807, Sep. 2016.

[33] K. Cumanan, Z. Ding, B. Sharif, G. Y. Tian, and K. K. Leung, "Secrecy rate optimizations for a MIMO secrecy channel with a multiple-antenna eavesdropper," *IEEE Trans. Veh. Technol.*, vol. 63, no. 4, pp. 1678–1690, May 2014.

[34] J. Steinwandt, S. A. Vorobyov, and M. Haardt, "Secrecy rate maximization for MIMO Gaussian wiretap channels with multiple eavesdroppers via alternating matrix POTDC," in *Proc. IEEE Int. Conf. Acoust., Speech Signal Process. (ICASSP)*, May 2014, pp. 5686–5690.

[35] S. A. A. Fakoorian and A. L. Swindlehurst, "Full rank solutions for the MIMO Gaussian wiretap channel with an average power constraint," *IEEE Trans. Signal Process.*, vol. 61, no. 10, pp. 2620–2631, May 2013.

[36] G. Scutari, F. Facchinei, and L. Lampariello, "Parallel and distributed methods for constrained nonconvex Optimization—Part I: Theory," *IEEE Trans. Signal Process.*, vol. 65, no. 8, pp. 1929–1944, Apr. 2017.

[37] G. Scutari, F. Facchinei, L. Lampariello, S. Sardellitti, and P. Song, "Parallel and distributed methods for constrained nonconvex optimization—Part II: Applications in communications and machine learning," *IEEE Trans. Signal Process.*, vol. 65, no. 8, pp. 1945–1960, Apr. 2017.

[38] S. Zhang and R. Zhang, "Capacity characterization for intelligent reflecting surface aided MIMO communication," 2019, *arXiv:1910.01573*. [Online]. Available: http://arxiv.org/abs/1910.01573

[39] S. P. Boyd and L. Vandenberghe, *Convex Optimization*. Cambridge, U.K.: Cambridge Univ. Press, 2014.

[40] T. Hu, J. Xiong, D. Ma, and Q. Shan, "Optimal and robust AN-aided precoding design for cognitive MIMOME wiretap channels," in *Proc. IEEE/CIC Int. Conf. Commun. China (ICCC)*, Aug. 2018, pp. 500–505.

[41] S. Iwata, T. Ohtsuki, and P.-Y. Kam, "A lower bound on secrecy capacity for MIMO wiretap channel aided by a cooperative jammer with channel estimation error," *IEEE Access*, vol. 5, pp. 4636–4645, 2017.

WEIHENG JIANG (Member, IEEE) received the Ph.D. degree in communication engineering from Chongqing University, Chongqing, China, in July 2015. He is currently an Assistant Professor with the School of Microelectronics and Communication Engineering, Chongqing University. His research interests include a broad range of areas from signal processing to wireless communications and networking, include 5G and beyond, big data algorithms, machine learning, and deep learning. He is also a Reviewer of the IEEE Transactions on Communications, the IEEE Transactions on Vehicular Technology, the IEEE Systems Journal, IEEE Access, and some other journals.
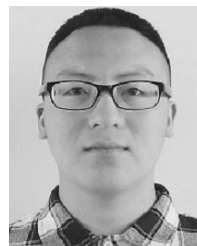
YU ZHANG received the B.E. degree in communication engineering from Chongqing University, Chongqing, China, in July 2018, where he is currently pursuing the master's degree with the School of Microelectronics and Communication Engineering. His research interests include 5G and beyond, deep learning, and the application of optimization technology in network resource allocation.

JINSONG WU (Senior Member, IEEE) is currently the Founder and the Founding Chair of the Technical Committee on Green Communications and Computing and the IEEE Communications Society. He is also the Founder and an Editor of Series on Green Communications and Computing Networks of the *IEEE Communications Magazine*. He was a Guest Editor of the IEEE Systems Journal, IEEE Access, the IEEE Journal on Selected Areas on Communications (JSAC), the *IEEE Communications Magazine*, the IEEE Wireless Communications, and *Computer Networks* (Elsevier). He is also an Area Editor of the JSAC Series on Green Communications and Networking. He has been on the Editorial Boards of a number of technical journals, such as the IEEE Communications Surveys and Tutorials, the IEEE Systems Journal, IEEE Access, the *International Journal of Big Data Intelligence*. He was the leading Editor and a coauthor of the comprehensive book *Green Communications: Theoretical Fundamentals, Algorithms, and Applications* (CRC, 2012).

WENJIANG FENG received the Ph.D. degree in electrical engineering from Chongqing University, Chongqing, China, in 2000. He is currently a Professor with the College of Communication Engineering, Chongqing University. His research interests include all aspects of MIMO communication, including limited feedback techniques, antenna design, interference management, full-duplex communication, cognitive radio, special mobile communication systems, and emergency communication. He is also a Senior Member of the China Institute of Communications. He is also a Peer-Review Expert of the Natural Science Foundation of China. He also serves as an Editorial Board Member of Data Communication, China.

YI JIN received the B.E. degree in communication and information engineering from the Nanjing University of Information Science and Technology, Nanjing, China, in 2005, and the Ph.D. degree in communication and information engineering from Southeast University, Nanjing, in 2013. He is currently with the Xi'an Branch of China Academy of Space Technology, Xi'an, China. His research interests include communication signal processing, satellite communication, and networking.

• • •